Advances in Colloid and Interface Science 326 (2024) 103137

Contents lists available at ScienceDirect

Advances in Colloid and Interface Science

journal homepage: www.elsevier.com/locate/cis

Historical Perspective

Recent advances on outstanding microwave absorption and electromagnetic interference shielding nanocomposites of ZnO semiconductor

Raghvendra Singh Yadav *, Ivo Kuřitka

Centre of Polymer Systems, University Institute, Tomas Bata University in Zlín, Trida Tomase Bati 5678, 760 01 Zlín, Czech Republic

ARTICLE INFO

Keywords:
ZnO semiconductor
Composites
Electromagnetic interference shielding
Microwave absorption

ABSTRACT

The electromagnetic interference shielding and microwave attenuation capabilities of ZnO semiconductor nanocomposites have recently been improved using a variety of approaches by correctly modifying their permittivity. To improve microwave attenuation, ZnO semiconductor nanostructures have been combined with graphene, multi-wall carbon nanotubes, metal nanoparticles and their alloys, two-dimensional MXene, spinel ferrite magnetic nanoparticles, polymer systems, and textiles. This paper covers the opportunities and constraints that these cutting-edge nanocomposites in the field of electromagnetic wave absorption encounter as well as the research progress of ZnO semiconductor-based nanocomposite. The structure-function relationship of electromagnetic wave absorption nanocomposites, design strategies, synthesis techniques, and various types of advanced nanocomposites based on ZnO semiconductor are also covered. In order to design and prepare high efficiency ZnO semiconductor based electromagnetic wave absorbing materials for use in applications of next-generation electronics and aerospace, this article can offer some useful ideas.

1. Introduction

The modern lifestyle is heavily reliant on electromagnetic (EM) radiation, which has a wide range of applications depending on its wavelength [1–3]. Microwaves and radio waves, which have frequencies lower than those in the far-infrared spectrum, are widely employed in broadcasting, information, and communication technologies to transmit signals [4]. Due to the rapid rise in mobile phone usage, the development of the internet of things (IoT), and the growing usage of a number of other electrical and electronic devices, high-frequency electromagnetic waves, also known as microwave and radiofrequency waves, are continuously emitted through a variety of antenna types all around us [5]. Electromagnetic radiation from nearby sources can combine and disrupt the regular functioning of adjacent electronic components. When two signals interact and produce unintentional changes, it is known as electromagnetic interference (EMI) [6]. EM interference (EMI) is the term used to describe this kind of coupling or interference. Electromagnetic interference (EMI) can cause electronic devices to malfunction or perform poorly. The growing reliance of modern civilization on computers, digital electronics, and low-voltage signal circuits has resulted in an increase in EMI-related issues [7]. For example, personal electronic devices must be switched off during takeoff and landing in order to prevent electromagnetic interference (EMI) from impairing the pilot's communication with ground stations or even interfering with the regular operation of the aircraft's instruments. Electromagnetic interference (EMI) can originate from natural phenomena like solar flares, thunder, and electrostatic discharge. It can also arise from nearby electronic devices that create electromagnetic waves as a result of flaw or design. Strong electromagnetic fields produced by MRI machines have the potential to interfere with nearby electrical devices, including medical ones [8]. Strong EM radiation used in broadcasting and telecommunications can be harmful to people's health over time. It can change the blood flow to the brain and can lead to serious illnesses including leukemia and brain tumors [9]. Fig. 1 shows a few potential electromagnetic wave sources as well as some potential interference-affected equipment. Thus, the urgent need to reduce harmful EM pollution and radiation drives the development of high-performance microwave absorption and EMI shielding materials in the GHz range [10,11].

Designed to act as a barrier, EMI shielding keeps away electromagnetic radiation that could otherwise interfere with communications and electronics [12]. Magnetic fields can easily interfere with some electrical

* Corresponding author.
E-mail address: yadav@utb.cz (R.S. Yadav).

https://doi.org/10.1016/j.cis.2024.103137
Received in revised form 14 February 2024;
Available online 21 March 2024

equipment because of the very low voltages and currents they use. The two basic ways to protect against EMWs are by absorption and reflection. Since the surrounding region may be harmed by the reflected EMWs, the absorption method is recommended for shielding from a safety standpoint. Therefore, EMI shielding-especially in the military and civil divisions-is one of the finest methods for protecting the environment and the health of living things from the harmful effects of electromagnetic waves [13–14].

Zinc oxide (ZnO) semiconductor nanoparticle, a type of superior multifunctional material, have exceptional physico-chemical characteristics such high chemical stability, high electrochemical coupling coefficient, wide radiation absorbance range, and high light stability [15]. It is one of the most widely used semiconductor metal oxide [16–17]. In fact ZnO exhibits a rare combination of excitonic stability and a high band gap energy of approximately 3.4 eV. It can be considered for light emission applications due to its high excitonic energy of approximately 60 meV [18]. ZnO is an n-type semiconductor whose intrinsic defects, such as oxygen vacancies and interstitial zinc atoms, are primarily responsible for its electrical conductivity. It is possible to increase electrical conductivity by doping with different group III or group VII elements [19]. Because of its strong pyroelectric and piezoelectric properties, ZnO is a good choice for applications including the manufacturing of piezoelectric sensors and mechanical actuators [20]. As a result of its great biocompatibility and antibacterial qualities, ZnO has also found widespread application in biosensing and biomedical applications [21].

Currently, materials based on ZnO provide ideal options for reducing electromagnetic wave pollution because of their superior dielectric loss characteristics [22]. It has been demonstrated that the electromagnetic wave absorption properties may be successfully modified by controlling the grain size, morphology, and microstructure of ZnO semiconductors by adjusting the preparation approach and also constructing creative nanocomposites [23]. Currently, most studies combine ZnO semiconductor with graphene, multi-wall carbon nanotube, metal nanoparticles and its alloys, two-dimensional MXene, spinel ferrite magnetic nanoparticles, polymer systems, textiles, etc. to acquire excellent microwave absorption properties. For example, Gaihua He et al. [24] reported superior electromagnetic wave absorption based on ZnO capped MnO_2 nanostructures. In comparison to pure ZnO or MnO_2, the compositions improved the electromagnetic wave attenuation performance, improve relative permittivity, and meet impedance matching requirements. A design guide for binary heterogeneous transition metal oxide dielectric-dielectric loss type electromagnetic wave absorption composites with improved microwave absorption performance over a wide frequency range is provided by heterogeneous nanostructures with large specific surface area and rich interfaces. Additionally, ZnO nanowires were used to modify three-dimensional reduced graphene oxide foam by Xin Liu et al. [25] for improved microwave absorption capabilities. Due to optimized impedance matching, increased polarizations, numerous residual oxygen functional groups, and defects of N doped reduced graphene oxide (N-RGO), the composite's electromagnetic wave absorption properties were improved.

This review article describes the recent research progress on ZnO semiconductor nanostructures and its nanocomposites for electromagnetic interference shielding and microwave absorber (Fig. 2). This is the first review of ZnO nanocomposites for microwave absorption and EMI shielding. More attention is paid to innovative nanocomposites such as ZnO-graphene based nanocomposites, ZnO-MXene based nanocomposites, ZnO-carbon nanotubes-based nanocomposites, ZnO-metal and its alloys-based nanocomposites, ZnO-spinel ferrite-based nanocomposites, ZnO-polymer based nanocomposites, ZnO-textile based nanocomposites and its designs strategies on the electromagnetic properties and electromagnetic wave absorption mechanisms. Finally, future research and development in ZnO based nanocomposites for electromagnetic absorption are discussed.

2. Electromagnetic wave absorption theory

The electromagnetic shielding and microwave absorber materials either interact with one of the oscillating electric and magnetic fields (i.e., electromagnetic waves) or with both, which results in interactions in the gigahertz range of the electromagnetic waves. The oscillation of the electromagnetic fields interacting with the material will produce a relative response, leading to the dissipation of the entire electromag-

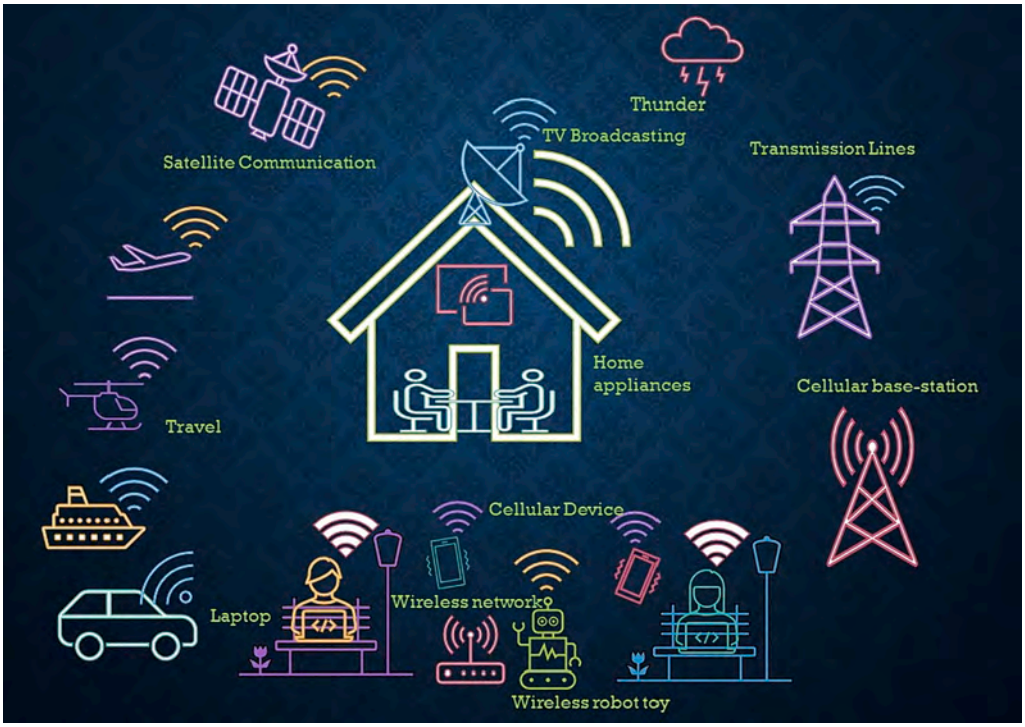

Fig. 1. Schematic illustration of the possible source of EMI and influenced devices.

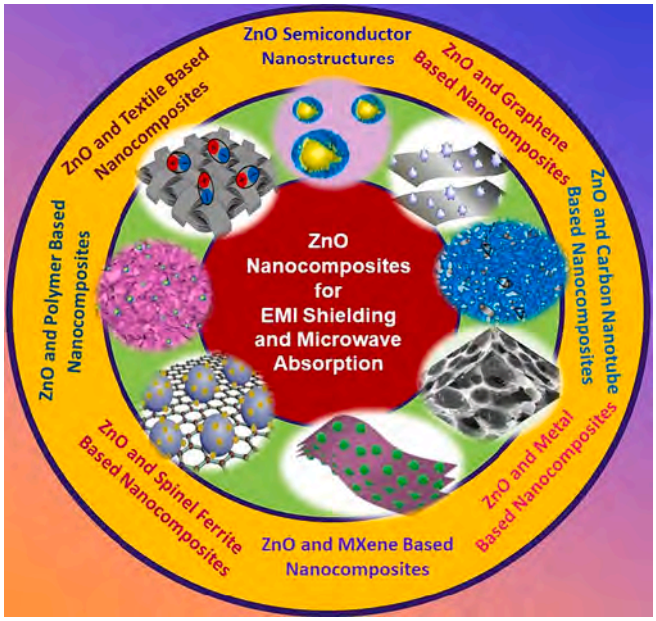

Fig. 2. Schematic illustration of ZnO nanocomposites for electromagnetic interference shielding and microwave absorption. Reproduced with permission from ref. [72]. Copyright 2016, Elsevier Publication. Reproduced with permission from ref. [85]. Copyright 2021, Elsevier Publication. Reproduced with permission from ref. [89]. Copyright 2022, Elsevier Publication. Reproduced with permission from ref. [105]. Copyright 2022, ACS Publication. Reproduced with permission from ref. [115]. Copyright 2020, Elsevier Publication. Reproduced with permission from ref. [116]. Copyright 2023, Elsevier Publication. Reproduced with permission from ref. [126]. Copyright 2020, ACS Publication.

netic waves. This interaction fits in Maxwell's eqs. [26]. According to Maxwell's equations, the bulk permittivity and permeability of materials that absorb electromagnetic wave energy determine their responses to electromagnetic waves, with the complex values representing an assessment of the materials' combined energy storage and dissipation [27]. The complex relative permittivity and permeability that profoundly affect the materials' capacity for absorption are expressed in following eqs. [28].

$$\varepsilon_r = \frac{\varepsilon}{\varepsilon_o} = (\varepsilon^{'} - i\,\varepsilon^{''})$$

$$\mu_r = \frac{\mu}{\mu_o} = (\mu^{'} - i\,\mu^{''})$$

The real components (ε' and μ') stand in for polarization and magnetization, which are related to the capacities for storing energy. The loss and attenuation properties are represented by the imaginary parts (ε'' and μ''), respectively [29].

2.1. Dielectric loss and conduction loss

The oscillatory polarity of the electric field produced by the electromagnetic waves initially causes the charge distribution of the material's particles. Intrinsic potential is created by the movement of electromagnetic waves through the material, which is different from its initial state [30]. Polarization is the term used to describe this phenomenon, which attenuates electromagnetic waves. The lossless interaction between the electromagnetic waves and material is quantified in this manner by the real part of permittivity ε', and imaginary part of permittivity ε'' can be thought of as the friction between the polarized particles that results in the energy conversion of electromagnetic waves into other types of energy [31]. In addition, the relaxation peak connected to the material's dielectric resonance, where energy dissipation is at its greatest, is described by the imaginary part of permittivity, ε''.

Polarization and conduction losses account for the majority of the dielectric loss [32]. In line with the free electron theory [33]:

$$\varepsilon^{''} \approx \frac{\sigma}{2\pi\varepsilon_o f}$$

where σ is the conductivity. Since higher conductivity σ results in a higher imaginary part of permittivity ε'', conduction loss σ is a significant contributor to dielectric loss and has a significant impact on the reflection coefficient. Due to the elastic nature of the associated motions and the low energy dissipation in the gigahertz range, electronic polarization and atomic polarization are ineffective [34]. Therefore, the dipole orientation polarization and interfacial polarization are the main cause of dielectric dispersion, which is very important to broaden the absorption bandwidth of the electromagnetic wave absorbers [35]. The orientation of a dipole polarization can influence the dielectric constant, and defects and functional groups in materials can amplify this effect. Dipoles cannot respond quickly to changing electric fields at high frequencies because they are bound charges and limited [36]. In heterogeneous systems, interfacial polarization and related relaxation are widespread. Space charge accumulates at the surface and is unevenly distributed, resulting in the formation of a macro dipole moment, which effectively reduces incident electromagnetic energy [37]. In order to describe the relaxation process and clarify the relationship between ε' and ε'', Debye's theory introduces Cole-Cole semicircles [38]:

$$\left(\varepsilon^{'} - \frac{\varepsilon_s + \varepsilon_\infty}{2}\right)^2 + (\varepsilon^{''})^2 = \left(\varepsilon_s - \frac{\varepsilon_s - \varepsilon_\infty}{2}\right)^2$$

where, the static dielectric constant is denoted as ε_s, and the dielectric constant at infinite frequency is denoted as ε_∞. If a polarization relaxation process exists based on Debye's dipole relaxation, the curve of ε' and ε'' will be a semicircle, denoted as the Cole-Cole semicircle, representing the Debye relaxation [39]. The strength of the polarization relaxation can be determined by counting the number and radius of semicircular curves. The semicircle will typically take on the shape of an arc when there are several relaxation processes. Additionally, the Cole-Cole curve's straight line at the end indicates the existence of conduction loss. Additionally, the following relationship is used to describe the frequency-dependent dielectric loss [40]:

$$\varepsilon^{''}(\omega) = \varepsilon_p^{''} + \varepsilon_c^{''} = (\varepsilon_s - \varepsilon_\infty)\frac{\omega\tau}{1+\omega^2\tau^2} + \frac{\sigma}{\varepsilon_{o\omega}}$$

where σ is the electrical conductivity, τ is the relaxation time, $\varepsilon_p^{''}$ is the polarization loss and, $\varepsilon_c^{''}$ is the conduction loss.

2.2. Magnetic loss

Magnetic materials will experience magnetization and reversal magnetization in an electromagnetic field. During these processes, the incident electromagnetic energy is converted to thermal energy and ultimately dissipates as magnetic loss. Magnetic loss is caused by resonances, including natural resonances, eddy current loss, and exchange resonances. By comparing the resonance peaks with an analysis of anisotropy fields, it is possible to determine the magnetic loss caused by the natural resonance, and this loss can be expressed as a function of the gyromagnetic ratio γ and the anisotropic field H_a [41]:

$$f_r = \frac{\gamma H_a}{2\pi}$$

where f_r is the resonance frequency. Due to the small size effect and binding effect when the particle size is in the nanoscale range, H_a will significantly increase. As a result, altering the anisotropic field helps to change the frequency. It makes sense to assume that natural resonance is what causes the resonance peaks at low frequencies [42]. A material

experiences eddy current loss when a changing magnetic field causes conduction current. This leads to the production of Joule heat [43]. The coefficient $C_o = \mu''(\mu')^{-2} f^{-1}$ can be used to analyze how eddy current contributes to magnetic loss, where, if C_o stays constant during variations in frequency (f), eddy current loss will be the only contributing factor [44]. When particles reach the submicron or nanometer scale, exchange resonance is typically ignored, and as particles get smaller, the exchange resonance frequency rises [45].

2.3. Impedance matching

The majority of the electromagnetic wave will be reflected at the surface of the absorbing material as a result of impedance mismatch [46–47]. Thus, attenuation of electromagnetic wave entering the absorbing material requires adequate impedance matching [48]. A mathematical model for linking the reflection coefficient Γ and transmission coefficient τ to the input parameters of permittivity and permeability in terms of the input impedance Z_{in} was developed by classical electromagnetic theory, as expressed in the following relation [49]:

$$\Gamma = \frac{Z_{in} - Z_o}{Z_{in} + Z_o}$$

$$\tau = 1 + \Gamma = \frac{2Z_{in}}{Z_{in} + Z_o}$$

$$Z_o = \sqrt{\frac{\mu_o}{\varepsilon_o}}$$

$$Z_{in} = \sqrt{\frac{\mu_r}{\varepsilon_r}}$$

where Z_o is the free-space impedance, μ_o is the free-space permeability, ε_o is the free-space permittivity, μ_r is the permeability of material, ε_r is the permittivity of material. The input impedance Z_{in} can also be evaluated by using electromagnetic parameters and the thickness of the material as expressed in the following relation [50]:

$$Z_{in} = Z_o \sqrt{\frac{\mu_r}{\varepsilon_r}} tanh\left(j\frac{2\pi f}{c} d\sqrt{\mu_r \varepsilon_r}\right)$$

In the above equation, f is the frequency of the electromagnetic wave, c is the speed of the light, and d is the absorber material thickness. According to the transmission line theory (TML), the reflection loss (RL) of a material can be measured under a normal incidence by using following eq. [51]:

$$RL = 20log|\Gamma| = 20log\left|\frac{Z_{in} - Z_o}{Z_{in} + Z_o}\right|$$

This equation is most frequently employed to express the material response despite some validity concerns. The value of the RL approaches to negative infinity as the reflection coefficient's value leans toward 1, and this is where the logarithmic function reaches its limit - ∞. This idea is known as impedance matching [52]. Perfect materials can completely absorb the incident microwave, therefore since Γ = 0, Z_{in} matches Z_0. However, the transmission coefficient τ will improve to almost 1, which indicates that there will be no dissipation of the microwave as it passes through the material. A delta-function method has also been widely used recently to assess the degree of characteristic impedance matching [53]:

$$|\Delta| = \left|sinh^2(Kfd) - M\right|$$

where the relative complex permittivity and relative complex permeability can be used to evaluate K and M:

$$K = \frac{4\pi\sqrt{\mu'\varepsilon'} * sin\left(\frac{\delta_e + \delta_m}{2}\right)}{c * cos\delta_e * cos\delta_m}$$

$$M = \frac{4\mu'\varepsilon' cos\delta_e * cos\delta_m \sqrt{\mu'\varepsilon'} * sin\left(\frac{\delta_e + \delta_m}{2}\right)}{(\mu' cos\delta_e - \varepsilon' cos\delta_m)^2 + \left[tan\left(\frac{\delta_e - \delta_m}{2}\right)\right]^2 (\mu' cos\delta_e + \varepsilon' cos\delta_m)^2}$$

when the delta value is near to 0, the impedance matching is ideal. Additionally, the value of |Δ| between 0.4 and 0 implies a good impedance match. It implies that the characteristic impedance will be better the larger the area of this small value is.

The following equation can be used to compute the attenuation coefficient's value [54]:

$$\alpha = \frac{\sqrt{2}\pi f}{c}\sqrt{(\mu''\varepsilon'' - \mu'\varepsilon') + \sqrt{(\mu''\varepsilon'' - \mu'\varepsilon')^2 + (\mu'\varepsilon'' + \mu''\varepsilon')^2}}$$

The equation shows that as μ'' and ε'' grow, the value of the attenuation coefficient also rises. However, an impedance mismatch results from too high μ'' and ε'' values. Since both the impedance matching and attenuation coefficient requirements must be fulfilled in order to achieve the best electromagnetic wave absorption performance, the values of μ'' and ε'' must be kept within a suitable range.

The effective absorption bandwidth (EAB) is the term used to describe the frequency band coverage when the RL value is less than −10 dB, which generally indicates that at least 90% of the electromagnetic waves are absorbed [55].

2.4. Geometric effect

Multiple electromagnetic waves reflections and scattering effects will occur in the gap structure at the micron scale. The electromagnetic wave propagation path will be effectively extended by this phenomenon, improving the electromagnetic wave absorption efficiency by expanding the window for electromagnetic wave attenuation loss. The other significant geometric effect for absorbing electromagnetic waves is interference elimination. The reflected electromagnetic waves in the metal-backed model will form at the air-absorber and absorber-metal back-plate heterogeneous interface.

$$d_m = \frac{n\lambda}{4} = \frac{nc}{4f_m\sqrt{|\mu_r||\varepsilon_r|}} \quad (n = 1, 3, 5, \ldots.)$$

The phase difference between these two reflected electromagnetic waves is precisely 180 degrees when the thickness of the electromagnetic wave absorber material (d_m) and the frequency of the incident electromagnetic waves (f_m) match the equation above. At this point, the interference elimination effect will start to manifest itself, allowing for the achievement of more impressive electromagnetic waves' attenuation absorption properties [56].

The distinct electromagnetic waves absorption property, it may be established, is determined by impedance matching, attenuation coefficient, dielectric loss, magnetic loss, multiple reflections and scattering, and interference elimination (Fig. 3).

3. Electromagnetic interference shielding

EMI shielding functions as a wall that is constructed to keep out electromagnetic radiation that may otherwise interfere with electronics and communications. Some electrical gadgets are easily affected by magnetic fields due to the extremely low voltages and currents they use. Absorption and reflection are the primary methods for electromagnetic wave protection [57]. Shielding efficiency (EMI SE), total shielding efficiency, or shielding effectiveness (SE_T) are terminology used to describe how well EMI shielding materials function.

It is a function of the logarithm of the ratio of the power P, electric E,

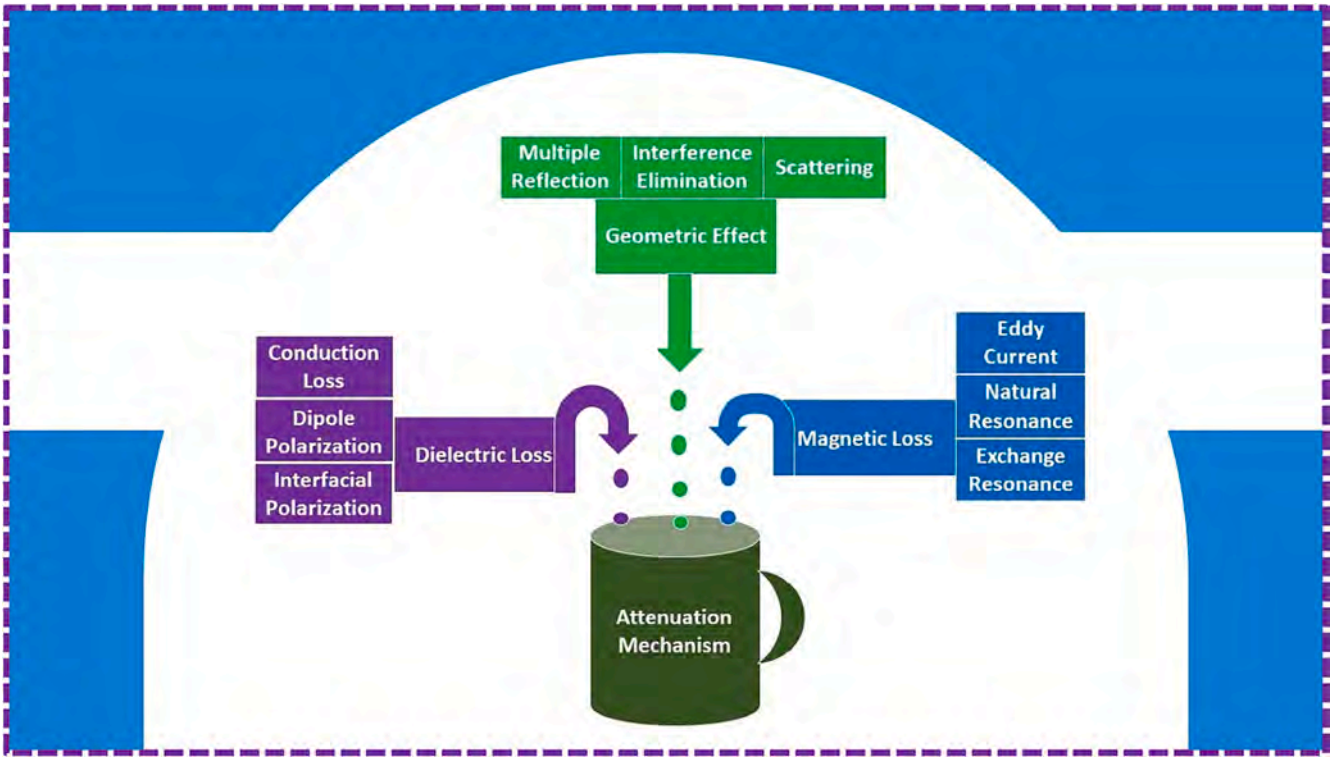

Fig. 3. The schematic illustration of electromagnetic waves attenuation mechanism.

or magnetic field strengths H before and after EM attenuation and is given in decibels (dB) as a measure of the material's capacity to block EM waves [58].

$$SE\ (dB) = 10log\left(\frac{P_T}{P_I}\right) = 20\ log\left(\frac{E_T}{E_I}\right) = 20log\left(\frac{H_T}{H_I}\right)$$

where I and T are incident and transmitted components.

Additionally, SE_T represents the total of the shielding effectiveness owing to reflection (SE_R), absorption (SE_A), and multiple internal reflections (SE_M) [59]:

$$SE_T = SE_R + SE_A + SE_M$$

SE_M no longer matters and can be disregarded in the equation above when SE_A is higher than 10 dB. The following equation gives the magnitude of reflection, which depends on surface conductivity [60]:

$$SE_R = -log_{10}\left(\frac{\sigma}{16\omega\varepsilon_o\mu_r}\right)$$

where σ is the total conductivity, μ_r is the relative permeability, ω is the frequency in Hz. As a result, the ratio of conductivity to permeability will be constant for a steady value of σ and μ_r, and SE_R will therefore be inversely proportional to frequency. However, absorption can diminish across the thickness and is determined by the following relation [61]:

$$SE_A = -8.68\ t\sqrt{\left(\frac{\sigma\omega\mu_r}{2}\right)}$$

where t is the thickness. Shielding mechanisms are linked to relative permittivity and permeability values because total conductivity is related to the permittivity. The SE of 20 dB is regarded as a benchmark for industrial and commercial applications of an EMI shielding material and can attenuate 99% of EM waves [62].

The scattering parameters, or "S-parameters," of a two-port network analyzer in the form of S_{11}, S_{22}, S_{21}, and S_{12} values are measured in order to experimentally determine the EMI SE values. The first and second subscripts denote the receiving and transmitting ports, respectively. For example, S_{21} stands for the scattering parameter value that was measured when electromagnetic waves were transmitted from port-1 and received at port-2. The following equations provide the coefficients of reflection (R), transmission (T), and absorption (A) using S-parameters [63]:

$$R = |S_{11}|^2 = |S_{22}|^2$$

$$T = |S_{21}|^2 = |S_{12}|^2$$

$$A = 1 - R - T$$

Using the measured parameters, the following formulas are used to obtain the SE_T, SE_R, and SE_A values:

$$SE_T = 10log\left(\frac{1}{T}\right) = 10log\left(\frac{1}{|S_{21}|^2}\right)$$

$$SE_R = 10log\left(\frac{1}{1-R}\right) = 10log\left(\frac{1}{1-|S_{11}|^2}\right)$$

$$SE_A = 10log\left(\frac{1-R}{T}\right) = 10log\left(\frac{1-|S_{11}|^2}{|S_{21}|^2}\right)$$

4. Recent progress on ZnO nanocomposites for EMI shielding and microwave absorption

4.1. ZnO semiconductor nanostructures

The microstructural parameters of ZnO crystals, such as their size, orientation, shape, aspect ratio, and crystalline density, have a significant impact on their electromagnetic properties. Recent research by Mei Cai et al. [64] revealed that ZnO nanoparticles may be easily manufactured and had high-performance electromagnetic microwave absorption. Zinc acetate dihydrate and ammonia water were used as the

primary ingredients in the sonochemical method that effectively produced ZnO nanoparticles (Fig. 4). Systematically, ZnO nanoparticles with various heat treatment processes were investigated for their dielectric and microwave absorption properties. With heat treatment at 120 °C for 8 h, the microwave absorption characteristics of the as-prepared ZnO particles were greatly improved. ZnO powders and paraffin were mixed consistently to create samples with a toroidal shape (outer diameter of 7.0 mm and inner diameter of 3.0 mm) for electromagnetic wave parameter measurements. With a thin thickness of 2.1 mm, the minimum reflection coefficient was −37.7 dB at 8.96 GHz (Fig. 4). Superior microwave absorption was achieved through the combination of oxygen vacancies, dipole polarization, and Debye relaxation.

Current research has focused in particular on the controlled synthesis of complex ZnO nanostructures with specified characteristics. ZnO nanostructures with hierarchical tree-like structures were created in one step and exhibit good microwave absorption, according to Renfu Zhuo et al. [65]. A large area of uniform and intriguing ZnO hierarchical tree-like nanostructures were synthesized by a simple one-step chemical vapor deposition (CVD) process using pure zinc powder and O_2 gas as source materials. Pure zinc powder and O_2 gas were used as the source materials for a straightforward one-step chemical vapor deposition (CVD) procedure that produced a large area of uniform and fascinating ZnO hierarchical tree-like nanostructures. While the reactions were occurring, ZnO nanowires was developed on the silicon substrate. Regular nanorods then uniformly grew on the ZnO nanowires to produce tree-like nanostructures when the flow rate of O_2 was increased. At 5 GHz and 4.0 mm in thickness, the composite with 40 vol% ZnO hierarchical tree-like nanostructures had a minimum reflection loss of −27.5 dB.

Further, ZnO nanotrees' microwave absorption characteristics were published by R. F. Zhuo et al. [66]. In a typical horizontal tube furnace, ZnO nanotrees were created using a two-step chemical vapor deposition procedure. In comparison to ZnO nanowire composite, ZnO nanotree composite exhibited superior microwave absorption characteristics, and the maximum absorption was improved as the concentration of the nanotrees in the composite rises (Fig. 5). At 4.2 GHz and 4.0 mm in thickness, the composites with 60 vol% ZnO nanotrees had a minimum reflection loss of -58 dB. Furthermore, crossed ZnO netlike micro−/nanostructures' microwave absorption properties were reported by Huifeng Li et al. [67]. Without the use of a catalyst, metal zinc and graphite powders were directly evaporated at 910 °C in Ar and O_2 to create three-dimensional ZnO micro/nanorod networks. According to calculations of the reflection loss (RL) of netlike structures and nanotetrapod-shaped ZnO, the minimum RL for a composite containing 50% ZnO netlike structures was −37 dB at 6.2 GHz and a thickness of 4.0 mm (Fig. 6). The 3D netlike ZnO structures' exceptional microwave absorption capabilities and distinctive shape point to possible uses for them in practical electromagnetic shielding technology.

Since the 3D porous ZnO architectures can not only provide the high surface accessibility and more free space to form the multi-interface reflection, but also offer point defects to cause another additional pathway for the highly efficient steady absorption of EM waves, hollow and open porous structures are desirable for the application in the shielding absorbing materials. Microwave absorption enhancement of porous and hollow ZnO spheres was reported by Yanyan Ren et al. [68]. One-pot solvothermal processing was used to create porous ZnO nanostructures. It was noticed that the synthetic porous and hollow ZnO calcined at 500 °C utilized as microwave absorbents had greater microwave absorption characteristics than the ZnO that had not been

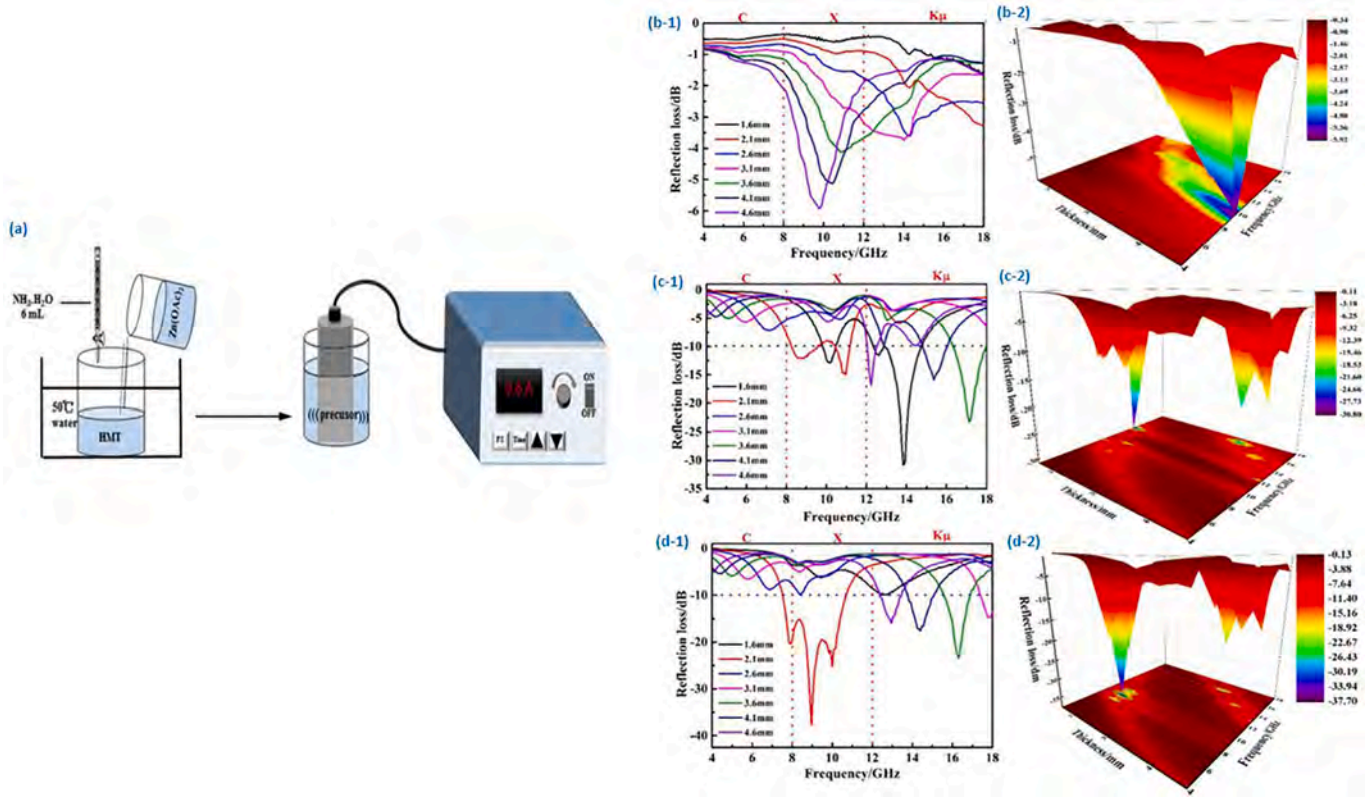

Fig. 4. (a) Schematic of preparation of ZnO. Reproduced with permission from ref. [64]. Copyright 2020, Elsevier Publication. (b-1) RL as function of frequency and thickness of ZnO; (b-2) The three-dimensional plots of the RL as function of frequency and thickness of ZnO; (c-1) RL as function of frequency and thickness of N-ZnO; (c-2) The three-dimensional plots of the RL as function of frequency and thickness of N-ZnO; (d-1) RL as function of frequency and thickness of H-N-ZnO; (d-2) The three-dimensional plots of the RL as function of frequency and thickness of H-N-ZnO. Reproduced with permission from ref. [64]. Copyright 2020, Elsevier Publication.

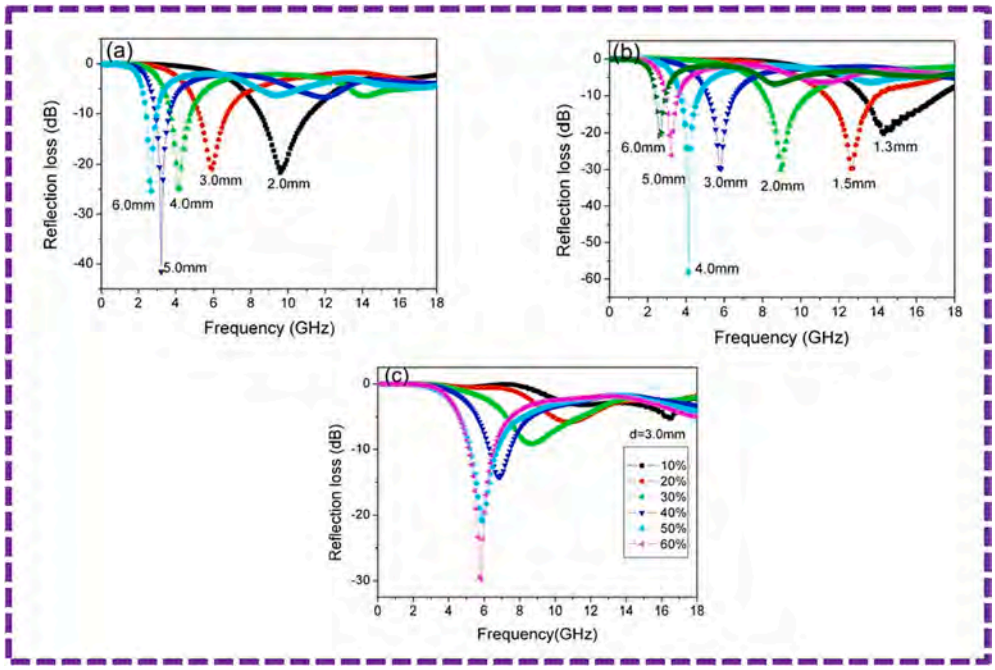

Fig. 5. Simulation of RL of ZnO nanotree composites with different thicknesses for (a) 50 vol% and (b) 60 vol% ZnO nanotrees, respectively. (c) RL of ZnO nanotree composite with a thickness of 3.0 mm of different loadings vs frequency. Reproduced with permission from ref. [66]. Copyright 2008, AIP Publication.

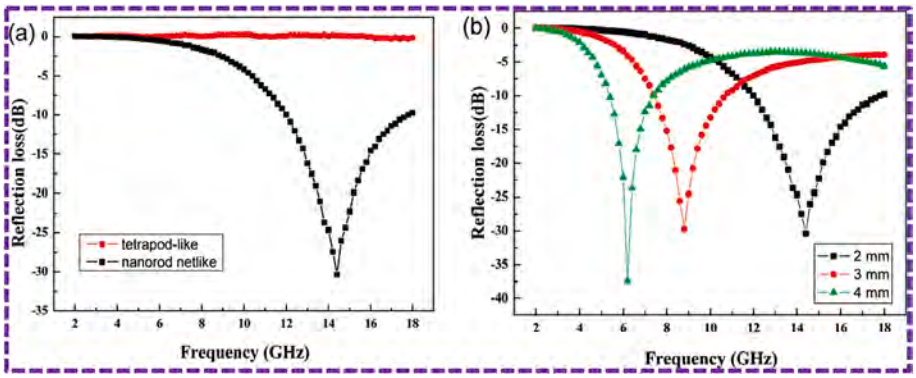

Fig. 6. (a) Simulation of reflection loss of 50 vol% ZnO nanotetrapod and 50 vol% ZnO netlike micro/nanostructures composites with a thickness of 2.0 mm. (b) Simulation of reflection loss of 50 vol% ZnO netlikes micro/nanostructures composite of different thickness. Reproduced with permission from ref. [67]. Copyright 2010, ACS Publication.

calcined and that had been calcined at 600 °C. With a thickness of 2.5 mm, the porous ZnO calcined at 500 °C reached a minimum RL value of -5.62 dB at 16.24 GHz. In addition, by calcining the hollow $ZnCO_3$, which was created using bubble CO_2 as a soft-template, Biao Zhao et al. [69] created the porous hollow structural ZnO with a straightforward, affordable process. The wax-composite with 25 wt% porous hollow ZnO had a minimum reflection loss of −36.3 dB at 12.8 GHz and a thickness of 4.0 mm. Further, a summary on recent progress on ZnO semiconductor nanostructures for EMI shielding and microwave absorption is tabulated in Table 1.

Table 1
Summary on recent progress on ZnO semiconductor nanostructures for EMI shielding and microwave absorption.

No.	Material	Frequency band	Optimum thickness	RL_{min} /SE_T	Ref.
1.	ZnO nanoparticles	4–18 GHz	2.1 mm	−37.7 dB	[64]
2.	ZnO nanostructures with hierarchical tree-like structures	0–18 GHz	4.0 mm	−27.5 dB	[65]
3.	ZnO nanotrees	0–18 GHz	4.0 mm	- 58 dB	[66]
4.	ZnO netlike structures	2–18 GHz	4.0 mm	−37 dB	[67]
5.	ZnO porous hollow structure	2–18 GHz	4.0 mm	−36.3 dB	[69]

4.2. ZnO and graphene based nanocomposites

Graphene or reduced graphene oxide (RGO), one of those conductive loss materials, has exceptionally high surface areas and carrier mobilities together with a wealth of defects and hydroxyl, epoxy, and carboxyl groups, making it very promising as a lightweight and highly effective microwave wave absorber [70]. The microwave absorption efficiency of RGO is still constrained by the agglomeration effects and inadequate impedance matching of pure RGO sheets. Decorating RGO with more microwave absorbers is the most viable solution, as concerns about the issues grow. It is well known that the importance of interfacial polarization in microwave attenuation can be increased by enlarging the

interface between various dielectrics in the absorber material [71]. The homogeneity and dispersion of composites contribute to the improvement of the interface of heterostructure. By doping ZnO on the surface of reduced graphene oxide (RGO), the electromagnetic wave impedance matching of RGO can be altered, which would lessen the reflection of electromagnetic waves. Wei Feng et al. [72] reported enhanced microwave absorption properties of reduced graphene oxide decorated with in-situ growing ZnO nanocrystals (Fig. 7). In order to improve the interfacial polarization of RGO/ZnO composites by an in-situ growing technique, this research team's work increases the interface in ZnO/RGO heterostructure by reducing the grain size of the ZnO nanocrystals and avoiding the aggregation of ZnO nanocrystals. Graphene oxide (GO) sheets absorbed zinc ions through interactions with functional groups in pure ethanol. The precursor of ZnO crystallized on GO sheets following the addition of hydroxyl ions and thermal treatment that reduced the GO. To evaluate the microwave absorption capabilities, wax was combined with RGO/ZnO nanocrystal composites at various mass fractions (5, 10, 15, 20 wt%). The sample's minimum RL value was −54.2 dB at 15.2 GHz when the loading concentration was 15 wt%, and its effective microwave absorption bandwidth was up to 6.7 GHz (from 11.4 GHz to 18 GHz) with the sample thickness of just 2.4 mm (Fig. 7). However, the microwave absorption capabilities decline as the loading concentration exceeds 15 wt%. It is well known that an excessively high permittivity affects impedance matching and causes a strong microwave reflection [73]. The impedance matching and sample microwave absorption are both hampered by the high loading concentration of RGO/ZnO composites. The expanded interface polarization at the RGO/ZnO interface, the improved impedance matching of RGO as a result of the adhering ZnO nanocrystals, the residual functional groups of the reduced graphene oxide, and the defects of ZnO formed in inert atmosphere are primarily responsible for the enhanced microwave properties of the composites.

Reduced graphene oxide-ZnO (rGO-ZnO) nanocomposite was easily synthesized by Ashwani Kumar Singh et al. [74] for superior electromagnetic interference (EMI) shielding application. ZnO nanoparticles between 40 and 50 nm were created in the first step of the synthesis using a straightforward reaction between zinc nitrate and sodium hydroxide (Fig. 8). The rGO/ZnO nanocomposite was made using as-synthesized ZnO nanoparticles and a solvothermal process mediated by ethylene glycol. The ZnO nanoparticles on the surface of the rGO exhibited a very high dispersion in the developed rGO/ZnO nanocomposite. The samples for the EMI shielding performance evaluations were hydraulic press-formed from the as-synthesized powder into rectangular pellets with dimensions of 15 × 8 × 1 mm^3. The rGO-ZnO nanocomposites' EMI shielding properties were examined, and it was found that the composite (SE_T ≈ 38 dB) displayed good shielding compared to its individual components (SE_T ≈ 22 dB for rGO and ≈ 4 dB for ZnO nanoparticles, respectively) (Fig. 8). The ZnO nanoparticles that have been formed across the surface of the rGO matrix to create the heterostructure with polarization centers may be responsible for these intriguing characteristics.

In a supporting framework made of reduced graphene oxide (RGO), zinc oxide nanoparticles (ZnO NPs) were immobilized using a straightforward one-step technique, according to Shouchun Bao et al. [75]. ZnO NPs performed a crucial function as a catalyst for the acceleration of GO deoxygenation as compared to a blank GO sample in a mild aqueous environment. GO sheets were reduced to RGO with ZnO NPs enclosed during this process, and a Zn-O-C linkage bond was established between the ZnO NP and RGO sheet. In terms of electromagnetic microwave absorption, the ZnO/RGO composite performed well, with a maximum reflection loss value of −67.13 dB at 3.2 mm thickness and an effective absorption bandwidth of 7.44 GHz at 2.8 mm.

It has been demonstrated that the microwave absorption properties may be successfully adjusted by controlling the morphology and microstructure of ZnO by changing the preparation approach. Using a hydrothermal process, Jun-Zhe He et al. [76] created a special structure of axiolitic ZnO rods wrapped in reduced graphene oxide and showed extremely effective microwave absorption. Due to the addition of axiolitic ZnO rods and the creation of unique structures, the composites demonstrated impressive microwave absorption capability with a minimum RL of −55.7 dB for a thickness of just 2.0 mm and an effective absorption bandwidth covering the whole Ku band (Fig. 9). Conductivity, interface polarization, and dipole polarization work in concert to increase the microwave attenuation capacity. The synergistic effect of dipole polarization, interface polarization and conductivity manifestly boost the microwave attenuation capacity. A study on the optimization, design, and microwave absorption characteristics of reduced graphene oxide/tetrapod-like ZnO composites was published by Long Zhang et al. [77]. Reduced graphene oxide (RGO) and tetrapod-like ZnO (T-ZnO) were mixed together to create a novel microwave absorption composite. Dielectric loss significantly increased with an increase in RGO content. However, the absorption peaks first rose and then fell. At 2.9 mm in thickness, the composites containing 5 wt% RGO and 10 wt% T-ZnO exhibited the best microwave absorption capabilities, and the corresponding minimum reflection loss was −59.50 dB at 14.43 GHz. The RGO's dielectric relaxation and polarization, the electronic polarization occurring at the needle-like tips of the T-ZnO, electrical conduction loss, and multiple scattering were primarily responsible for the remarkable microwave absorption capabilities.

The superior properties of the three-dimensional (3D) structure graphene materials, such as their low density, high porosity, large specific surface area, and excellent electrical conductivity, make them

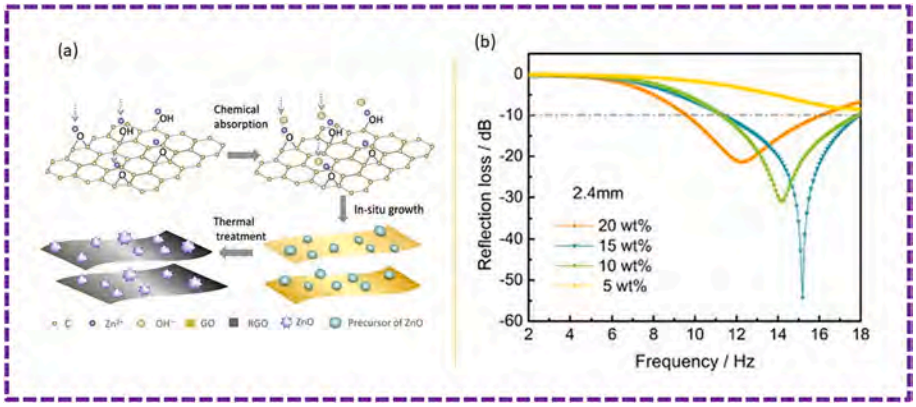

Fig. 7. (a) A schematic illustration of the formation process of ZnO nanocrystals/RGO composites. Reproduced with permission from ref. [72]. Copyright 2016, Elsevier Publication. (b) Reflection loss calculated for the samples loading different content of RGO/ZnO composites with a thickness of 2.4 mm. Reproduced with permission from ref. [72]. Copyright 2016, Elsevier Publication.

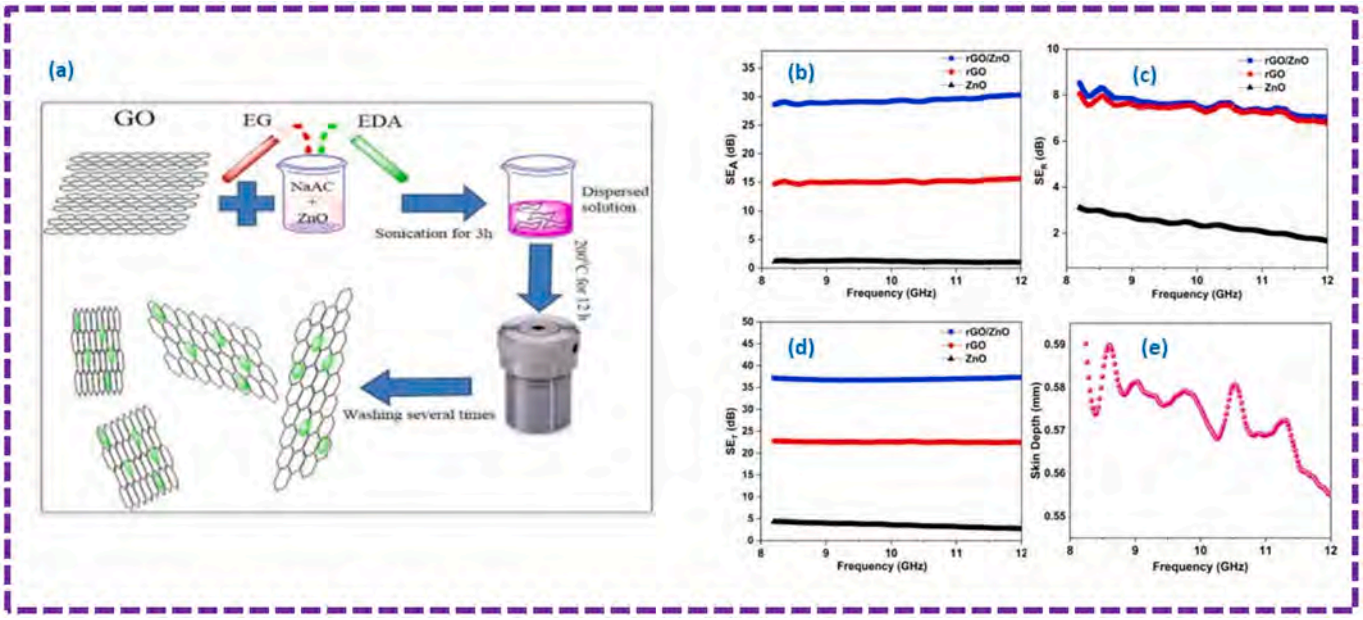

Fig. 8. (a) Schematic illustration of the synthesis of rGO/ZnO nanocomposite. Reproduced with permission from ref. [74]. Copyright 2019, Elsevier Publication. Variation of SE_A (b) SE_R(B), and SE_T(c) of rGO, ZnO nanoparticles, and rGO/ZnO nanocomposite (d) variation of skin depth of rGO/ZnO nanocomposite. Reproduced with permission from ref. [74]. Copyright 2019, Elsevier Publication.

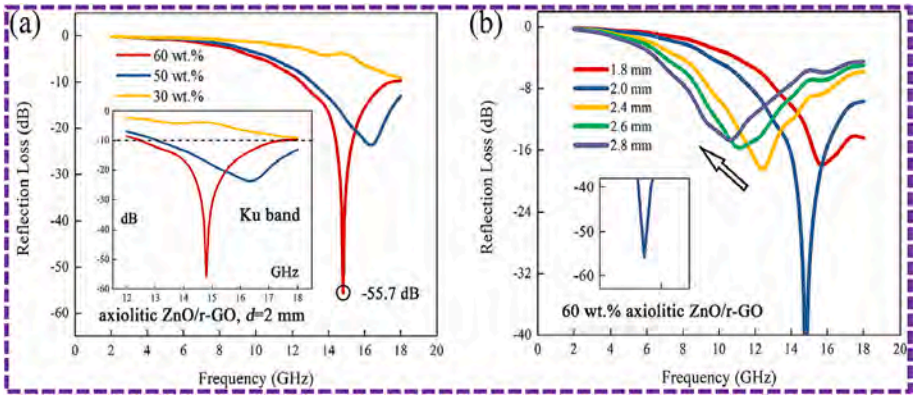

Fig. 9. (a) Reflection loss of axiolitic ZnO/r-GO with different mass ratios at 2.0 mm thickness; (b) Reflection loss of axiolitic ZnO/r-GO with 60 wt% mass ratio at different thickness. Reproduced with permission from ref. [76]. Copyright 2019, Elsevier Publication.

desirable and promising candidates for the development of a portable and effective microwave absorber [78]. Sen Yang et al. [79] used a novel and simple two-step synthetic technique that combined modified template-assisted preparation and in situ crystallization method in an aqueous solution to create a distinctive structure of 3D graphene/ZnO composite incorporating 3D graphene with shuttle-like ZnO. The shuttle-shaped ZnO nanoparticles were uniformly scattered on and incorporated into 3D graphene without any aggregation, according to morphology study, which was advantageous for enhancing the interfacial polarization. The RL surpassing −10 dB were recorded throughout the frequency range spanning from 12.98 to 17.06 GHz at a given thickness of 1.5 mm, and a minimum reflection loss of - 48.05 dB was obtained at 11.71 GHz with a thickness of 1.82 mm.

For improved microwave absorption capabilities, Changqing Song et al. [80] proposed 3D reduced graphene oxide foam modified with ZnO nanowires. By using a direct freeze-drying and hydrothermal procedure, a flexible and high-performance electromagnetic absorbent material was created from 3D hierarchical reduced graphene oxide (RGO) foams embellished with in-situ generated ZnO nanowires (ZnOnws). In addition to substantially decreasing RGO agglomeration and composite density, the distinctive structure also significantly improved the impedance match, dielectric loss, and inner scattering, leading to improved microwave absorption performance. The complex permittivity could be controlled by changing the RGO foam concentration, which also provided the ZnOnws/RGO foam with a tunable EM wave absorption property. To create the samples for microwave absorption, the ZnOnws/RGO foam and poly (dimethylsiloxane) solution were combined, which were then impregnated in vacuum for 30 min and then cured at 80 °C for 4 h. The ZnOnws/RGO foam/PDMS composite, when RGO foam was 0.8 mg/mL, achieved a minimum reflection loss value of −27.8 dB at 9.57 GHz with a thickness of 4.8 mm and a broad effective absorption bandwidth of 4.2 GHz encompassing the entire X band (8.2–12.4 GHz).

A high porosity, broad surface area, and tunable electromagnetic property can be achieved by heat treating graphene-like materials, which is a cost-effective, environmentally friendly, and scalable approach to increase their microwave absorption capacity. In recent years, researchers are paying a lot of attention to thermally expanded RGO (TERGO), which is produced by heating and expanding GO [81]. The porous structure of TERGO is identical to that of expanded graphite

(EG). It's interesting to note that TERGO has additional benefits in addition to its porous structure, such as: (i) the residual oxygen functional groups on TERGO can improve the conduction loss of electromagnetic waves. As free ions are drawn to the surface of graphene by the oxygen functional groups, oxides are formed, enhancing the interfacial polarization of the absorbent material [82]; (ii) RGO has superior impedance matching since it has a lower permittivity than graphite [83]; Additionally, (iii) TERGO has substantially smaller pores than EG, which causes higher microwave scattering and reflection. Microwave absorption characteristics of TERGO/ZnO porous composites produced by the method of heat treatment and hydrolysis process, which were easy to make and had a more uniform porous structure, were reported by Xin Liu et al. [84]. The interfacial polarization and impedance matching of the composites were enhanced by the development of ZnO on the TERGO sheets, which also enhanced their microwave absorption capabilities. With an effective absorption bandwidth (EAB) of 4.2 GHz, covering the whole x-band (8–12 GHz), and an RL_{min} of −19 dB at 10.0 GHz, the produced composites demonstrated good microwave absorption at 3.9 mm thickness.

ZnO/ZnO nanocrystal-modified rGO foam composites for microwave absorption application were designed logically, according to Xin Liu et al. [85]. These composites were created utilizing the hydrothermal and freeze-drying methods, and they have a variety of morphologies and mass ratios. The aggregation of rGO was effectively prevented by the growth of ZnO between the rGO sheets, and the ZnO nanocrystals developed and were dispersed uniformly on the surface of the rGO sheets. Due of the higher polarization loss, the composite with an 8:1 ZnO/rGO mass ratio showed greater permittivity. With an effective absorption bandwidth (EAB) in the frequency ranges of 8.7–11.1 and 11.5–12.4 GHz, an RL_{min} of −21 dB at 11.5 GHz, and a thickness of 3.4 mm, it displayed good capabilities as a microwave absorption material. Due to the composite's foam structure, appropriate impedance matching, improved polarization, capacitor-like structure, residual oxygen functional groups, and defects in the rGO sheets, it exhibited good microwave absorption performance (Fig. 10). In addition, a summary on recent progress on ZnO and graphene-based nanocomposites for EMI shielding and microwave absorption is tabulated in Table 2.

Table 2
Summary on recent progress on ZnO and graphene based nanocomposites for EMI shielding and microwave absorption.

No.	Material	Frequency band	Optimum thickness	RL_{min} /SE_T	Ref.
1.	ZnO nanocrystals/ RGO composites	2–18 GHz	2.4 mm	−54.2 dB	[72]
2.	rGO/ZnO nanocomposite	8.2–12 GHz	1 mm	38 dB	[74]
3.	ZnO/RGO	2–18 GHz	3.2 mm	−67.13	[75]
4.	Axiolitic ZnO rods wrapped in RGO	2–18 GHz	2.0 mm	−55.7 dB	[76]
5.	RGO and tetrapod-like ZnO (T-ZnO)	8–12 GHz	2.9 mm	−59.50 dB	[77]
6.	graphene with shuttle-like ZnO	1–18 GHz	1.82 mm	−48.05 dB	[79]
7.	ZnO nanowires/RGO foam	8.2–12.4 GHz	4.8 mm	−27.8 dB	[80]
8.	ZnO/ZnO nanocrystal-modified rGO foam	8.2–12.4 GHz	3.4 mm	−21 dB	[85]

4.3. ZnO and other carbon source material based nanocomposites

Recently, due to their exceptional physicochemical properties, carbon materials, particularly multi-wall carbon nanotubes (MWCNTs), have garnered a lot of attention. The nanocomposites of MWCNTs exhibit a low percolation threshold and good dielectric loss due to their high conductivity and one-dimensional tubular structure. The resulting nanocomposites may have improved electromagnetic interference (EMI) shielding and microwave attenuation due to the addition of MWCNTs with ZnO semiconductor nanoparticles. Multi-wall carbon nanotubes decorated with ZnO nanocrystals for a highly effective microwave absorber were reported by Ming-Ming Lu et al. [86]. ZnO nanocrystals were used to decorate multi-wall carbon nanotubes (ZnO@MWCNTs) during a mild solution-process synthesis. The dielectric loss was also influenced by the polarization at the ZnO-MWCNT and ZnO-ZnO interfaces as well as the defect dipoles resulting from oxygen vacancies in ZnO. The composites had a minimum RL of −20.7 dB at a sample thickness of 2.5 mm. By creating more interfaces, the created ZnO@MWCNT hybrids demonstrated greater dielectric loss and extremely effective microwave absorption.

According to Xiaohui Li et al. [87], ZnO nanocrystals embedded in CNTs have numerous polarization sites that contribute to their improved microwave absorption performance. This research team described a novel confined space synthesis method for coating CNTs with a polypyrrole (PPy) layer in order to embed ultra-fine ZnO crystals made of zeolite imidazole framework-8 (ZIF-8) into the CNTs. Through a novel confined space synthesis, ultra-fine ZnO derived from ZIF-8 was uniformly dispersed and tightly embedded in multi-wall carbon nanotubes (C-ZnO@CNTs). By adjusting its thickness, C-ZnO@CNTs showed improved microwave absorption capacity with an RL value of up to -48.2 dB and an effective bandwidth of 14.9 GHz. This result can be attributed to the local charge field and the resulting interfacial polarization loss as well as conductive loss, as shown by electronic

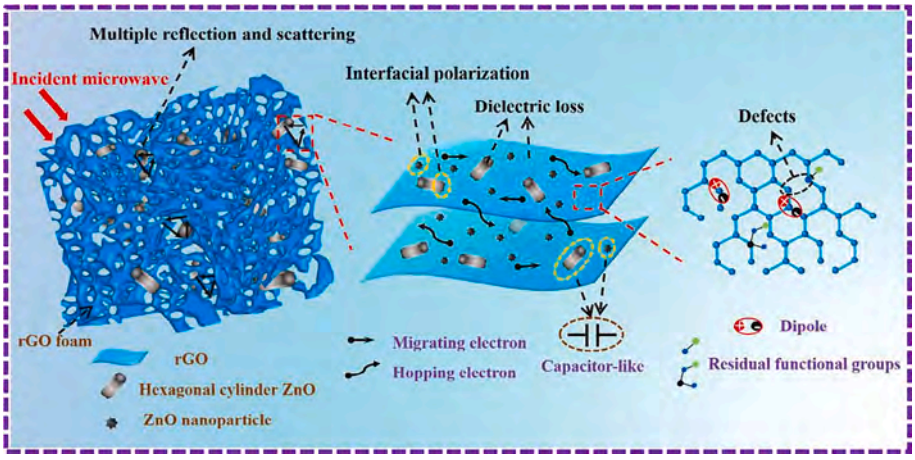

Fig. 10. Schematic for the microwave absorption properties mechanisms of hexagonal cylinder ZnO/rGO modified by ZnO nanocrystals foam composites. Reproduced with permission from ref. [85]. Copyright 2021, Elsevier Publication.

holography. The distinctive architecture encourages multiple scattering and reflection to dissipate energy. The ultra-fine ZnO, on the other hand, contributes to interfacial polarization, dipole polarization, and improved synergistic effects and impendence matching in the composites (Fig. 11), which resulted in a superior microwave absorption performance.

The porous carbon has a special channel structure with a large surface area that lowers density, creates conductive networks for good conductive loss, increases the channel distance for the incident wave to allow for more scattering and multiple reflections, and gives the medium more chances to absorb and attenuate microwave energy [88].

Innovative lightweight carbon foam (CF) embellished with zinc oxide nanofibers (ZONF) was created by Anushi Sharma et al. [89] for high-performance electromagnetic interference (EMI) shielding. Prior to being decorated by ZONF using the electrospinning technique, the CF was first created from the phenolic resin using the polyurethane (PU) foam impregnation method, followed by carbonization (Fig. 12). Different electrospinning times, i.e. 15, 30, and 45 min, were selected for the ZONF on CF. With a thin thickness of 2 mm, the neat CF had a low density of 0.25 g/cm^3, a high porosity of 83.5%, and an EMI shielding of 23.2 dB at 8.2 GHz. ZONF was applied to the CF for 45 min, resulting in the CF-ZONF45, which had a thickness of 2 mm, a porosity of 81.2%, and the highest EMI shielding of 58.6 dB at 8.2 GHz. Due to a higher dielectric constant, better impedance matching, and interfacial polarization, the decoration of ZONF on CF improves absorption performance. Additionally, a connected ZONF network and decorated foam with high open porosity are helpful in attenuating the EM wave with greater absorption.

The enhanced microwave absorption of ZnO/porous carbon was demonstrated by Qi Chen et al. [90]. The production of zinc oxide nanoparticles (ZnO NPs) embedded in porous carbon from the reaction of sucrose and zinc nitrate hexahydrate was described as a simple solvent-free process. This research team used zinc nitrate hexahydrate as a foaming agent along with sucrose to create ZnSuc in a solvent-free environment. The distinctive hierarchically porous carbon composite with plentiful ZnO NPs was created through additional heat treatment. Numerous polar OH groups in the bio-based sucrose support the transport function through reversible binding. The prerequisite for the uniform mixing of zinc ions and sucrose is provided by bio-based sucrose due to its high affinity for divalent zinc ions. By adjusting the ratio of zinc nitrate hexahydrate and sucrose, the structural properties and ZnO NPs content were controlled. The final products were labeled as ZnO/C-x, where x = 0.5, 1, 2, and 3, respectively, and were made using four different weight ratios of zinc nitrate hexahydrate to sucrose: 1:2, 1:1, 2:1, and 3:1. With a frequency of 14.5 GHz and a thin thickness of 2 mm, the best-designed ZnO/C-2 carbon material showed the strongest absorption of −41.7 dB, and its widest effective absorption was close to 6 GHz (12.2–17.8 GHz), as shown in Fig. 13. This easily accessible high-performance porous composite material had notable interface polarization, conductive loss, and impedance matching, emphasizing its capacity for attenuation.

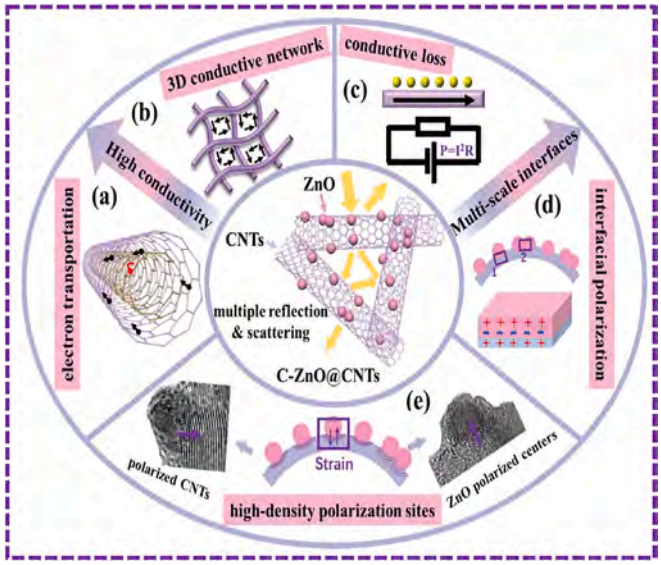

Fig. 11. Microwave absorption mechanisms for C–ZnO@CNTs. Reproduced with permission from ref. [87]. Copyright 2019, RSC Publication.

Additionally, carbon nanofibers embedded with ZnO nanocrystals were found to have improved electromagnetic wave absorption properties, according to Jinyang Li et al. [91]. The C/ZnO nanofiber composites carbonized at 700 °C can achieve a maximum RL of −61.91 dB at 11.44 GHz under the corresponding thickness of 2.59 mm, and the effective absorption bandwidth reached 5.60 GHz. The graphite-like carbon nitride/zinc oxide heterojunction for microwave absorption was reported by Cong Chen et al. [92]. By placing the hierarchical ZnO flowers on 2D g-C_3N_4, it was possible to develop a g-C_3N_4/ZnO heterojunction with controlled components. The ratio of the components between g-C_3N_4 and ZnO was optimized to achieve the maximum polarization. The ideal heterojunction had a maximum effective absorption region of 5.3 GHz under 1.5 mm, an RL_{min} of - 43.3 dB at 2.0 mm thickness, and a broad EM absorption ability. Moreover, a summary on recent progress on ZnO and other carbon source material-based nanocomposites for EMI shielding and microwave absorption is tabulated in Table 3.

4.4. ZnO and metal and metal alloys based nanocomposites

The ability of the materials to absorb microwave energy is generally improved by the interactions between magnetic loss and dielectric loss as well as by interfacial polarization. The characteristics of metal (magnetic)/ZnO composites for microwave absorption, however, have been the subject of relatively little research. Ni is currently the subject of intensive research in the field of microwave absorption because of its high permeability at GHz frequency ranges, simple preparation, and low cost [93]. A simple design of a ZnO nanorod-Ni core-shell composite with dual peaks to adjust its microwave absorption properties was reported by Jiushuai Deng et al. [94]. In their study, Ni/ZnO composites were made using a simple one-pot hydrothermal method. By adjusting the solvents, the morphologies of the Ni/ZnO composites were modulated. Absolute ethanol, 1,2-propanediol, and glycerol were used to create the Ni/ZnO composites, which were designated as Samples A, B, and C, respectively. It was discovered that the morphologies of the Ni/ZnO composites were influenced by the solvents. The sizes and shapes of the Ni/ZnO products were greatly influenced by the solvents' viscosity ratings. The core-shell Ni@ZnO produced in the ethylene glycol-containing solvent demonstrated superior microwave absorption capabilities (Fig. 14). With a 2.2 mm thick absorber, the optimal reflection loss minimum was −30.2 dB at 10.8 GHz. With a low thickness of 1.7–2.5 mm, the effective bandwidth (RL less than −10 dB, or 90% microwave dissipation) could be modulated in the frequency range of 9.6–14.3 GHz. An effective impedance match, high attenuation capacity, an antenna receiver mechanism, and interfacial polarization were said to be the causes of the superior absorption.

Cu/ZnO core/shell structures for improved microwave absorption were reported to self-assemble in one pot under the influence of dual ligands by Yi-Feng Cheng et al. [95]. The easy one-pot methods were used to create the spherical Cu/ZnO core/shell (sample 1) and rod-shaped Cu/ZnO core/shell (sample 2) nanocomposites. The heating rate at 220–250 °C can be adjusted to change the size and aspect ratio of the resulting Cu/ZnO core/shell nanocomposite. When compared to pure ZnO, both Cu/ZnO core/shell nanocomposites performed significantly better at microwave absorption, particularly the rod-shaped one (Fig. 15). With a thickness of 3.5 mm, the maximum absorption was as strong as - 40.98 dB at 6.54 GHz. Due to the anisotropy effect, the aspect

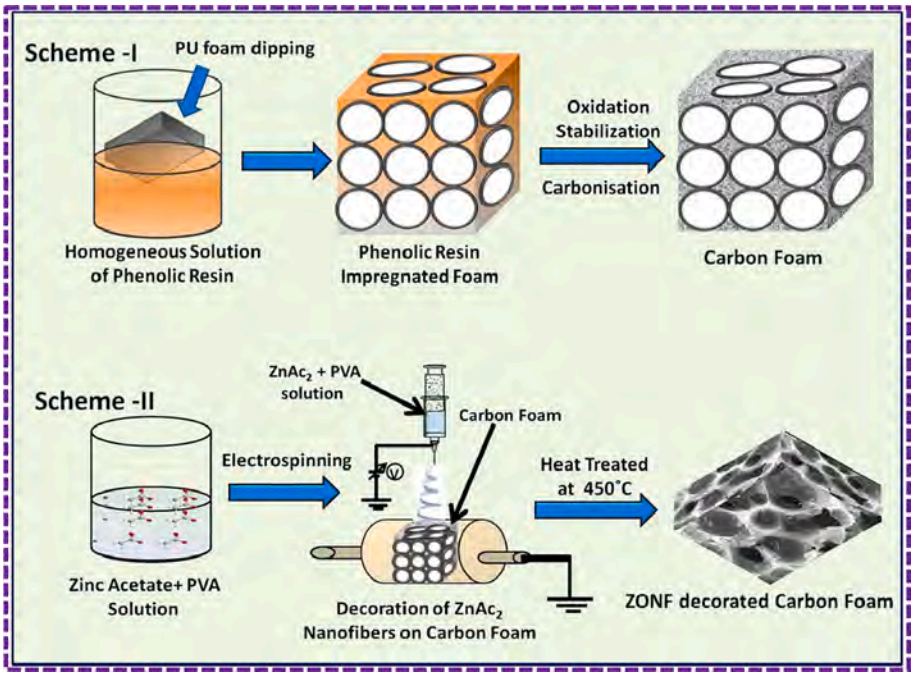

Fig. 12. Schematic presentation for the synthesis of carbon foam (Scheme-I) and decoration of ZONF on carbon foam (Scheme-II). Reproduced with permission from ref. [89]. Copyright 2022, Elsevier Publication.

ratio of hybrid Cu/ZnO nanocrystals plays a beneficial role in improving microwave absorption.

By simply heating a mixture of boron and ZnO powders at 1300 °C via chemical vapor deposition (CVD), Bo Zhong et al. [96] reported a new simple method to fabricate Zn/ZnO core-shell nanocables on a relatively large scale. The nanocables had a diameter of between 30 and 200 nm and a length of tens of microns. The shell was a 3–10 nm thick epitaxially grown ZnO layer, and the core was a single Zn crystal. The composite's maximum reflection loss, which was −23 dB at 13.22 GHz, was exceptional when compared to composites containing other ZnO-related nanostructures (Fig. 16).

Tunable Co/ZnO/C@MWCNTs based on carbon nanotube-coated MOF were reported by Zirui Jia et al. [97] and have excellent microwave absorption properties. By pyrolyzing ZnCo-MOF@MWCNTs (MOF@M), this research team demonstrated how to make Co/ZnO/C@MWCNTs (CZC@M) composites. This research team discovered that the MWCNT addition significantly affects the composites' structural and electromagnetic properties. CZC@M exhibited a wider effective absorption bandwidth, a lower reflection loss value, and a thinner matching thickness with a 50% addition of MWCNTs. Its distinct multi-component composite structure dissipated microwaves more efficiently than the corresponding single component or derivative, whose RL value was - 41.75 dB at a thickness of 2.4 mm and the maximum absorption bandwidth was 4.72 GHz at a thickness of 2.2 mm. Further, ZnO/nitrogen-doped carbon nanocomplex with controlled morphology for extremely effective electromagnetic wave absorption was reported by Zhen Yu et al. [98]. ZIF-8 precursors with yolk-shell and hollow architectures were prepared via one-step chemical etching. It was possible for the resultant ZnO/NC nanocomplexes to keep their micro/nanostructures during pyrolysis at 700 °C and 800 °C. Furthermore, the samples with hollow structures showed superior microwave absorption compared to those with yolk-shell construction; at 3.1 mm thickness, the EAB was 4 GHz, the RC_{min} was −52.4 dB, and the mass fraction of H-ZnO/NC-800 absorber was 15 wt%.

In both the civil and military sectors, significant microwave absorption performance at high temperatures is highly desired. With its high complex permeability, exceptional frequency stability, and superior Curie temperature, the magnetic alloy flaky-FeCo has an intriguing potential for use at high temperatures. The metal powder, however, is frequently easily oxidized by raising temperatures and has an excessively high conductivity that leads to poor impedance matching. In order to create a powerful material with significant and stable microwave absorption property at the temperature range of 298 K–573 K, Kangsen Peng et al. [99] created a ZnO coated flaky FeCo alloy. ZnO's coating effect significantly increases the oxidation resistance of FeCo at high temperatures. This research group noticed RL_{min} of −31.1 dB at 373 K and − 22.8 dB at 573 K for developed FeCo@ZnO composite material. FeCo/ZnO composite nanofibers for broad-spectrum, high-efficiency microwave absorption have been reported by Jingnan Yang et al. [100]. Through electrospinning, followed by calcination, hydrogen reduction; FeCo/ZnO NFs, a novel nanofibrous absorber made of FeCo alloy and ZnO nanoparticles was created. With a thin matching layer of just 1.3 mm, the minimum RL was achieved −83.4 dB at 12.8 GHz, and the EAB was as wide as 8 GHz (from 10.0 to 18 GHz). The developed FeCo/ZnO NFs exhibited exceptional microwave absorption properties at a thin coating thickness of just 1.3 mm, taking advantage of the benefits of their distinctive hierarchical structure as well as the good synergistic effect between magnetic FeCo alloy and dielectric ZnO.

Due to their unique atomic structure and composition, layered double hydroxides (LDHs) are predicted to be a superior electromagnetic wave (EMW) absorber. The creation of a 1D heterostructure NiCo@C/ZnO nanorod with improved microwave absorption was demonstrated by Jianwei Wang et al. [101]. This research team created NiCo@C/ZnO composites by first designing heterostructure NiCo-LDHs@ZnO nanorods and then heat treating them. At a matching thickness of 2.0 mm, the EAB_{max} value was 6.08 GHz, and the RL_{min} value was −60.97 dB at a matching thickness of 2.3 mm. The main factor influencing EMW's excellent attenuation properties was the interaction of magnetic and dielectric losses. In addition, a summary on recent progress on ZnO and metal and metal alloys-based nanocomposites for EMI shielding and microwave absorption is tabulated in Table 4.

4.5. ZnO and MXene based nanocomposites

Due to its innovative two-dimensional (2D) layered structure, high specific surface area, high electrical conductivity, and plenty of terminal

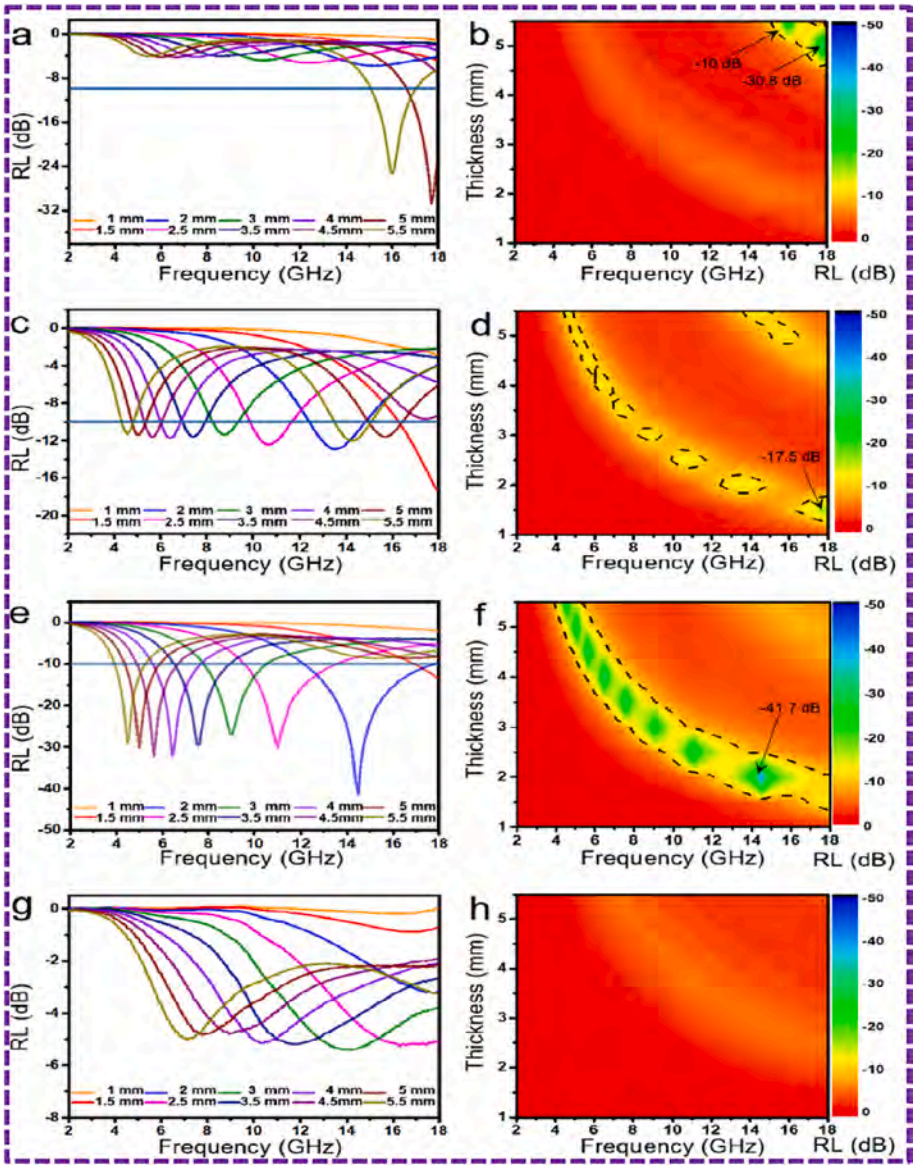

Fig. 13. RL versus frequency at various thicknesses for ZnO/C-0.5 (a, b), ZnO/C-1 (c, d), ZnO/C-2 (e, f), ZnO/C-3 (g, h). Reproduced with permission from ref. [90]. Copyright 2023, Elsevier Publication.

Table 3
Summary on recent progress on ZnO and other carbon source material-based nanocomposites for EMI shielding and microwave absorption.

No.	Material	Frequency band	Optimum thickness	RL_{min} /SE_T	Ref.
1.	ZnO@MWCNTs	8.2–12.4 GHz	2.5 mm	−20.7 dB	[86]
2.	C-ZnO@CNTs	2–18 GHz	3.0 mm	−48.2 dB	[87]
3.	ZnO/porous carbon	2–18 GHz	2 mm	−41.7 dB	[90]
4.	carbon foam (CF) embellished with zinc oxide nanofibers (ZONF)	8.2–12.4 GHz	2 mm	58.6 dB	[89]
5.	carbon nanofibers embedded with ZnO nanocrystals	2–18 GHz	2.59 mm	−61.91 dB	[91]
6.	g-C_3N_4/ZnO	2–18 GHz	2.0 mm	−43.3 dB	[92]

functional groups, $Ti_3C_2T_x$ MXene has potential for use as a microwave absorber [102,103]. The primary method for creating MXenes is to selectively etch A layers from the MAX phases, a large family of phases with more than 70 members. MXene is a type of dielectric loss absorber that primarily realizes dielectric loss as an electromagnetic wave loss due to its good dielectric characteristics. MXene has issues with impedance mismatching, a constrained microwave absorption bandwidth, and subpar microwave absorption performance because of its high permittivity [104]. As a result, inorganic metal oxides are frequently added to MXene in recent years to enhance microwave absorption capability. For instance, ZnO/MXene nanocomposites were prepared, and their performances were reported by Yufei Huang et al. [105]. This study team used an in situ composite approach to create a variety of ZIF-8/MXene microwave-absorbing materials, which were subsequently annealed under vacuum to create porous ZnO/MXene dielectric loss composites (Fig. 17). The ZnO/MXene composite annealed at 600 °C (Zn^{2+}/MXene = 2:1) has the highest microwave absorption capability, according to experimental observation in this work. The effective absorption bandwidth was 3.47 GHz from 13.49 to 16.96 GHz, and the minimum reflection loss was −34.31 dB at 8.8 GHz

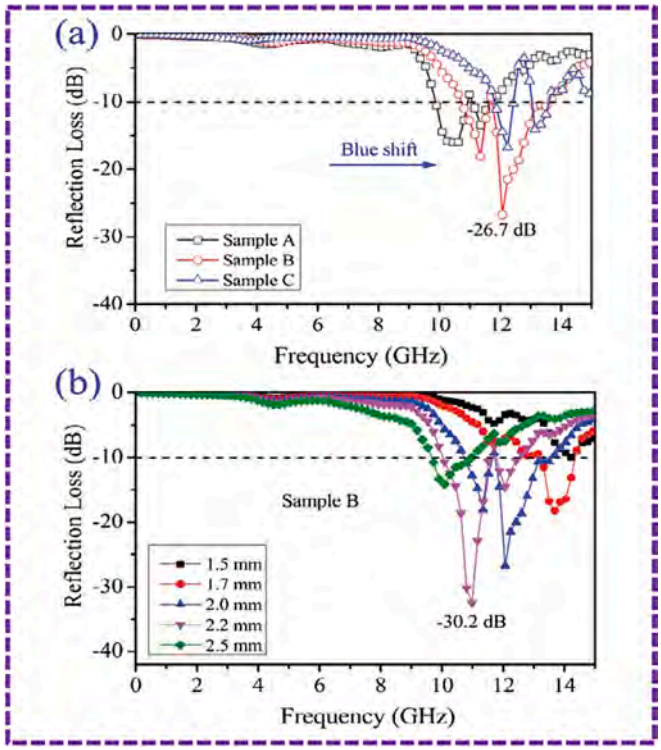

Fig. 14. (a) Reflection loss (RL) of the different Ni/ZnO composites with a thickness of 2.0 mm and (b) RL of the core–shell Ni@ZnO (Sample B) composite with various thicknesses. Reproduced with permission from ref. [94]. Copyright 2017, RSC Publication.

(Fig. 17). The 3D porous structure of ZnO, which aids in the attenuation of electromagnetic waves, and the inclusion of ZnO, which results in optimal impedance matching, are credited with the device's exceptional microwave absorption capability.

Hierarchical $Ti_3C_2T_x$@ZnO hollow spheres with superior microwave absorption were described by Yan-Qin Wang et al. [106]. Through the use of in-situ self-assembly and template sacrificial techniques, the biomimetic urchin-like $Ti_3C_2T_x$@ZnO hollow microspheres were created. The ZnO nanospines principally "shield" the incident electromagnetic wave in the urchin-like hollow spheres, while the $Ti_3C_2T_x$ hollow spheres also "conduct and process" the electromagnetic wave that the ZnO spines are unable to dissipate. Because of this, the urchin-like $Ti_3C_2T_x$@ZnO hollow spheres displayed exceptional electromagnetic wave performance with absorption as high as −57.4 dB and effective absorption band as wide as 6.56 GHz. Therefore, high-performance electromagnetic absorption composites can be created by constructing orientated ZnO nanospines, highly conductive $Ti_3C_2T_x$ cores, hollow structures, gradient impedance, and hierarchical urchin-like heterostructures.

A fabrication of urchin-like ZnO-MXene nanocomposites for high performance electromagnetic absorption was reported by Yue Qian et al. [107]. Through the use of a straightforward coprecipitation technique, a new urchin-like ZnO-$Ti_3C_2T_x$ nanocomposite was created. The ZnO-$Ti_3C_2T_x$ nanocomposite had a maximum reflection of −26.30 dB at 17.4 GHz, which was significantly better than that of the reported MXene materials. By altering the ZnO growth duration, the EM wave absorption performance in the range of 14.0–18.0 bands may be efficiently managed.

For excellent microwave absorption, Mingyue Kong et al. [108] created Co/ZnO/$Ti_3C_2T_x$ composites produced from metal-organic frameworks. Metal ions serve as the nodes of metal organic frameworks (MOFs), which are joined by organic ligands. MOFs have drawn a lot of interest in many study domains due to their benefits of high porosity, large specific surface area, tunable pore size, and topological

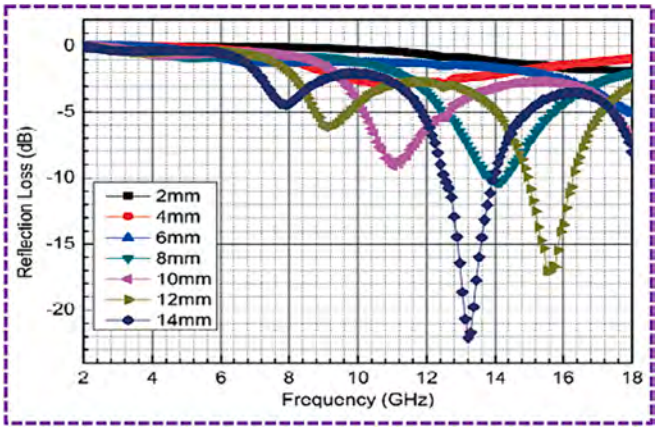

Fig. 16. Simulation of the reflection loss of the Zn/ZnO nanocable–paraffin composite with different thicknesses. Reproduced with permission from ref. [96]. Copyright 2015, RSC Publication.

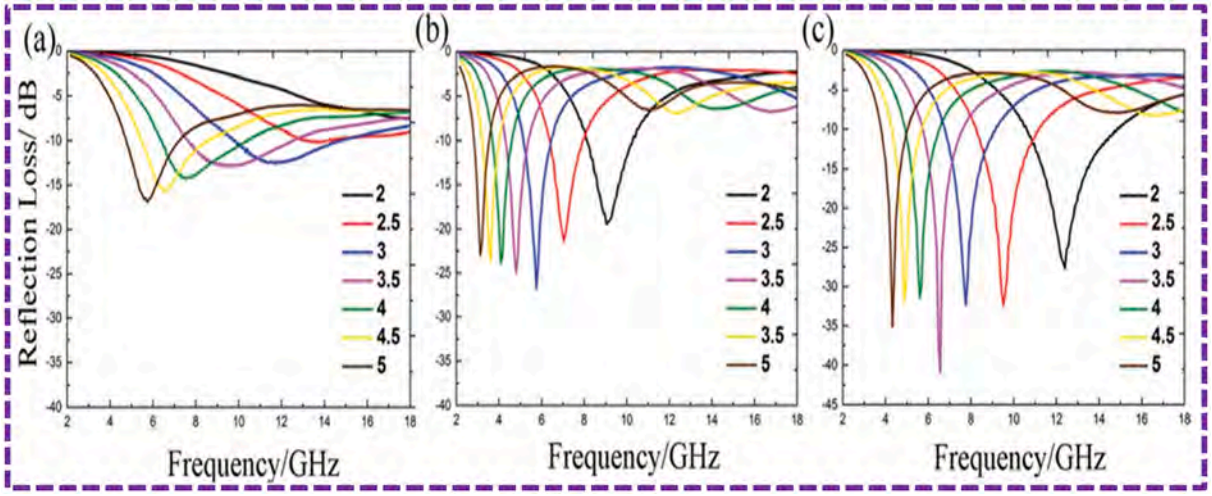

Fig. 15. Microwave reflection loss curves of (a) p-ZnO, (b) sample 1 and (c) 2 in the series of thicknesses: 2.0 mm, 2.5 mm, 3.0 mm, 3.5 mm, 4.0 mm and 5.0 mm, respectively. Reproduced with permission from ref. [95]. Copyright 2016, RSC Publication.

Table 4
Summary on recent progress on ZnO and metal and metal alloys-based nanocomposites for EMI shielding and microwave absorption.

No.	Material	Frequency band	Optimum thickness	RL_{min} /SE_T	Ref.
1.	Ni/ZnO composites	0.1–15 GHz	2.2 mm	−30.2 dB	[94]
2.	rod-shaped Cu/ZnO core/shell	2–18 GHz	3.5 mm	−40.98 dB	[95]
3.	Co/ZnO/C@MWCNTs	2–18 GHz	2.4 mm	−41.75 dB	[97]
4.	H-ZnO/NC-800	2–18 GHz	3.1 mm	−52.4 dB	[98]
5.	FeCo/ZnO composite nanofibers	2–18 GHz	1.3 mm	−83.4 dB	[100]
6.	NiCo@C/ZnO composites	2–18 GHz	2.3 mm	−60.97 dB	[101]

structure variety. Through self-assembly, a two-dimensional hetero-bimetallic (Zn, Co)-based MOF was formed on a layered $Ti_3C_2T_x$, and after a subsequent annealing procedure, the Co/ZnO/$Ti_3C_2T_x$ composites were created (Fig. 18). The best reflection loss value −44.22 dB could be achieved at a thickness of 2.4 mm when the annealing temperature was 750 °C, and the greatest effective absorption bandwidth was 5.28 GHz. Dielectric loss, magnetic loss, many reflections, and scattering are thought to be the causes of the microwave absorption mechanism (Fig. 18). The carbon framework created during the calcination of MOF and MXene has many interfaces between the Co and ZnO nanoparticles in the material, which can cause various interface polarizations and significantly increase the material's ability to improve dielectric loss. The incident microwaves are scattered and reflected numerous times as a result of the material's unique structure, consuming the microwave energy. The introduction of defects and heteroatoms, which might shift the position of the dipolar and increase the loss of dipolar polarization. The conduction loss is increased by the presence of carbon, Co, and ZnO particles embedded in the carbon. Finally, the structure's magnetic Co nanoparticles produce magnetic losses. In addition, a summary on recent progress on ZnO and MXene based nanocomposites for EMI shielding and microwave absorption is tabulated in Table 5.

4.6. ZnO and spinel ferrite based nanocomposites

Numerous research revealed that ferrite and ZnO together improved the complex dielectric parameters, optimized impedance matching and may significantly improve electromagnetic wave absorption. For example, three-dimensional (Fe_3O_4/ZnO)@C double-core@shell porous nanocomposites with improved broadband microwave absorption were reported by Xun Meng et al. [109]. By using a solution self-propagating combustion method, heat treatment, phenolic polymerization, and a subsequent in-situ carbothermal reduction process, the 3D (Fe_3O_4/ZnO)@C double-core@shell porous nano composites were created. It was discovered that adjusting the zinc content can alter how well the nanocomposites absorb microwaves. The effective absorption bandwidth of the double-core@shell nanocomposite was 6.4 GHz with 2 mm thickness and 7.11 GHz with 1.9 mm thickness when the molar ratio of Zn to Fe was 1:2. The double-core@shell nanocomposite, which had a Zn:Fe ratio of 1:1, had a wideband effective absorption of 6.5 GHz and an efficient absorption bandwidth of 3.4 GHz, and a minimum RL value of - 40 dB at 15.31 GHz (Fig. 19). The electromagnetic wave (EMW) absorption performance is enhanced by the dielectric loss caused by the carbon shell (multiple interfacial polarization, dipole and defect polarization), the magnetic loss (eddy current loss and magnetic resonances) primarily produced by the Fe_3O_4 core, and the dielectric loss caused by the ZnO core (Fig. 19). The foam-like absorber's porous structure offers a large number of channels for the EMW's scattering and propagation,

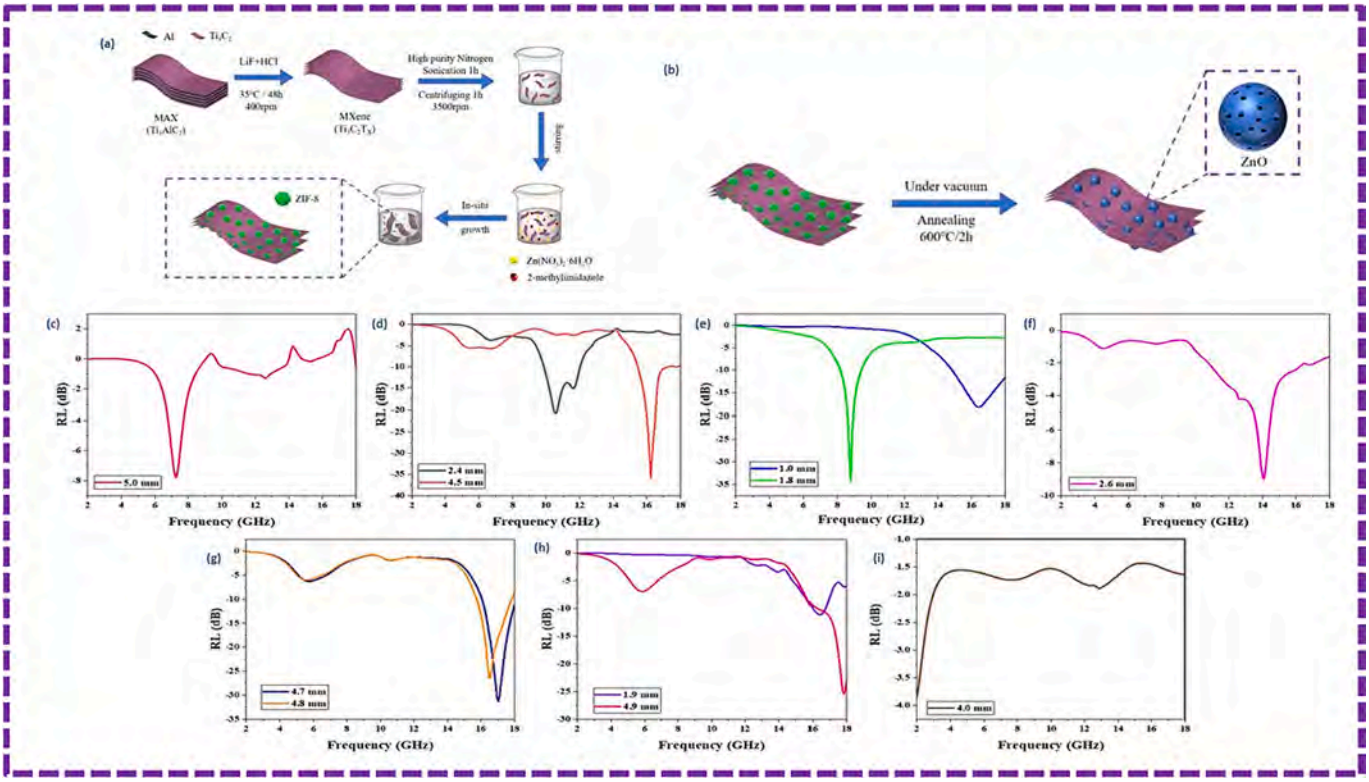

Fig. 17. (a) Synthesis Process of the ZIF-8/MXene Nanocomposite; (b) Preparation Process of the ZnO/MXene Nanocomposite. Reproduced with permission from ref. [105]. Copyright 2022, ACS Publication. RL values of (c) ZIF-8 and (d − h) a series of ZnO/MXene: the mass ratio of Zn^{2+}/MXene = (d) 1:1; (e) 2:1; (f) 3:1; (g) 1:2; and (h) 1:3 at various thicknesses (600 °C). (i) RL values of MXene without annealing. Reproduced with permission from ref. [105]. Copyright 2022, ACS Publication.

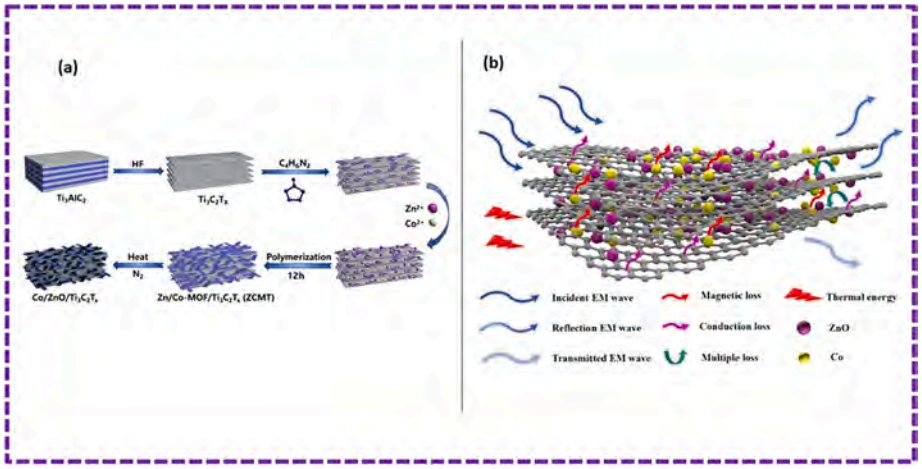

Fig. 18. (a) Schematic illustration of the fabrication process of the Co/ZnO/$Ti_3C_2T_x$. Reproduced with permission from ref. [108]. Copyright 2020, Elsevier Publication. (b) The illustration of the microwave absorption mechanism for the Co/ZnO/$Ti_3C_2T_x$. Reproduced with permission from ref. [108]. Copyright 2020, Elsevier Publication.

Table 5
Summary on recent progress on ZnO and MXene based nanocomposites for EMI shielding and microwave absorption.

No.	Material	Frequency band	Optimum thickness	RL_{min} /SE_T	Ref.
1.	ZnO/MXene nanocomposites	2–18 GHz	1.8 mm	−34.31 dB	[105]
2.	urchin-like $Ti_3C_2T_x$@ZnO hollow spheres	2–18 GHz	2.0 mm	−57.4 dB	[106]
3.	urchin-like ZnO-MXene nanocomposites	10–18 GHz	4.0 mm	−26.30 dB	[107]
4.	Co/ZnO/$Ti_3C_2T_x$	2–18 GHz	2.4 mm	−44.22 dB	[108]

which improves microwave attenuation. The proper ZnO composition and the cooperative action of the magnetic Fe_3O_4 core, conductive carbon shell, and ZnO can produce the optimal impedance values for the absorbers.

It is very important to use various approaches to create a special structure in order to enhance the electromagnetic wave absorption capabilities of absorbing materials for application in crucial domains. Wei Ma et al. [110] announced Fe_3O_4 nanoparticle-decorated ZnO nanorod-based microflowers for electromagnetic wave absorption. The hydrothermal method and annealing procedure were used to create three-dimensional (3D) ZnO nanorods that had sphere-shaped Fe_3O_4 nanoparticles added to give them distinctive microflower-like shapes and high-performance microwave absorption (Fig. 20). When the composites contained 11.3 wt% Fe_3O_4 as the filler, the best reflection loss (RL) value was −36.2 dB at 9.35 GHz with an absorber thickness of just 2.7 mm, and the corresponding absorption bandwidth was 4.02 GHz (6.81–10.83 GHz) in the range of 2–18 GHz. The ideal concentration of Fe_3O_4 nanoparticles and the increased polarization of the interface between ZnO nanorods and Fe_3O_4 nanoparticles established a material's superior electromagnetic wave absorption property. Further, the distinctive structure of ZnO/Fe_3O_4 composites can be attributed for the good compatibility and synergistic effect between Fe_3O_4 and ZnO.

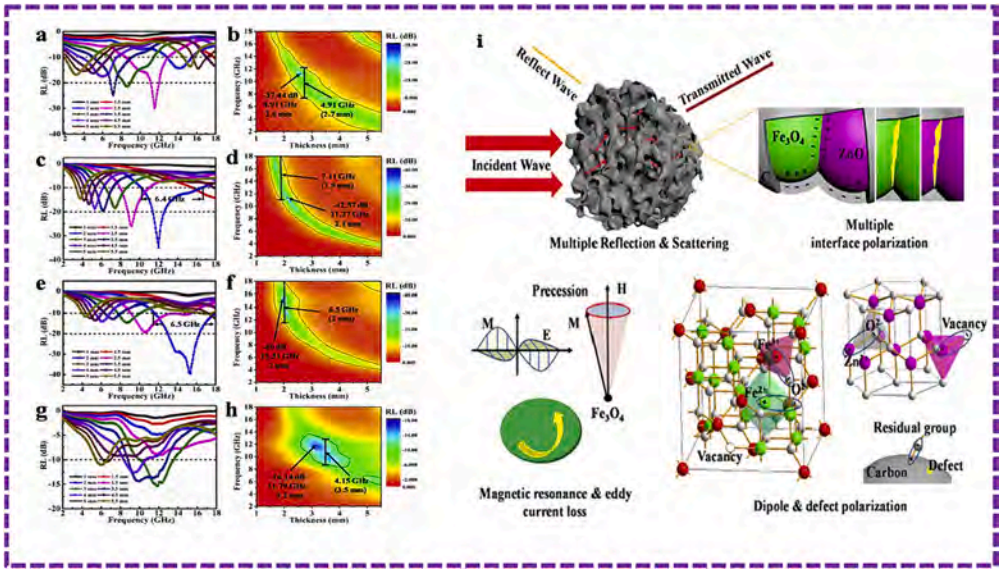

Fig. 19. Reflection loss values of the (Fe_3O_4/ZnO)@C nanocomposites at different thicknesses of 1–5.5 mm. (a and b): FZC1, (c and d): FZC2, (e and f): FZC3, (g and h): FZC4. Reproduced with permission from ref. [109]. Copyright 2020, Elsevier Publication. (i) Schematic representation of the EMW absorption mechanisms for 3D (Fe_3O_4/ZnO)@C double-core@shell nanocomposites. Reproduced with permission from ref. [109]. Copyright 2020, Elsevier Publication.

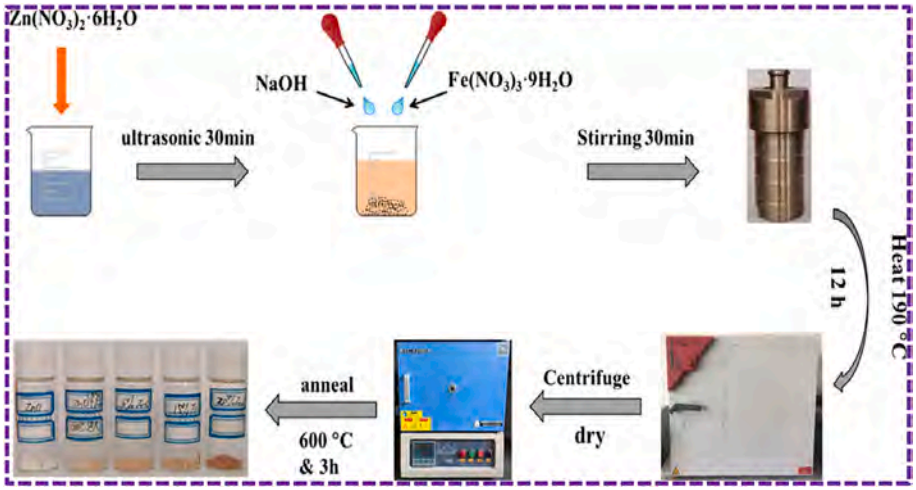

Fig. 20. Synthesis schematic illustration for ZnO/Fe_3O_4 nanorods. Reproduced with permission from ref. [110]. Copyright 2020, ACS Publication.

Furthermore, after heterogeneously growing with a ZnO nanoshell, Zhijiang Wang et al. [111] found improved microwave absorption of Fe_3O_4 nanocrystals. Heterogeneous nucleation on Fe_3O_4 nanocrystals resulted in the formation of a ZnO shell through the process of hydrothermal synthesis. The ZnO nanoshell coating significantly improves the material's capacity for microwave absorption. Fe_3O_4 nanocrystals alone previously had a minimum reflection loss of −3.31 dB; this was enhanced to −22.69 dB, with an effective absorption band covering the frequency range of 10.08 to 15.97 GHz. The findings showed that the dielectric property as well as the oxidation environment and distribution of Fe ions on the surface of Fe_3O_4 were both altered by the decorating of the dielectric ZnO shell. This effectively balances the nanomaterials' permeability and permittivity and makes it easier to impedance match the microwave absorber in free space. As a result, compared to Fe_3O_4 nanocrystals alone, the microwave absorption of the Fe_3O_4@ZnO nanohybrids was greatly enhanced.

Moreover, Yu-Lan Ren et al. [112] produced quaternary nanocomposites with good electromagnetic absorption capabilities made of graphene, Fe_3O_4@Fe Core@Shell, and ZnO nanoparticles. The G/Fe_3O_4@Fe/ZnO quaternary nanocomposites were synthesized, in which Fe_3O_4@Fe core/shell nanoparticles and ZnO nanoparticles were uniformly deposited on the graphene. The G/Fe_3O_4@Fe/ZnO quaternary nanocomposites were prepared, which consisted of Fe_3O_4@Fe core/shell nanoparticles and ZnO nanoparticles with uniform deposition on the graphene. The ternary nanocomposites' EM wave absorption capabilities were further enhanced after ZnO nanoparticles were deposited on them. The quaternary nanocomposites have multiple interfaces and triple junctions, which considerably improved their EM absorption capabilities. The quaternary nanocomposites' minimum RL value was −38.4 dB at 5 mm thickness, and the absorption bandwidth with RL values less than −20 dB reached up to 7.3 GHz (Fig. 21). The improved EM wave absorption was attributed to enhanced Debye relaxation process, the synergistic effects between the magnetic and dielectric losses of the quaternary nanocomposites, and the charge-carrier transfer between Fe_3O_4 and ZnO.

Pengfei Yin et al. [113] reported hierarchical ZnO flakes co-decorated with CoFe/$CoFe_2O_4$ and rGO for enhanced electromagnetic wave absorption. The magnetic CoFe/$CoFe_2O_4$ nanoparticles, ZnO flakes, and rGO were combined to create the CoFe/$CoFe_2O_4$/ZnO/rGO composites, which were then calcined in a vacuum environment after being aged simply (Fig. 22). The final samples were designated as S1, S2, S3, and S4, respectively, in accordance with the amounts of GO added, which were 0 g, 0.015 g, 0.025 g, and 0.035 g. The generated S3 sample at 2.5 mm has a broader effective absorption band (EAB) (7.66 GHz) than those of S1 (2.88 GHz at 2.5 mm), S2 (5.86 GHz at 3.0 mm), and S4

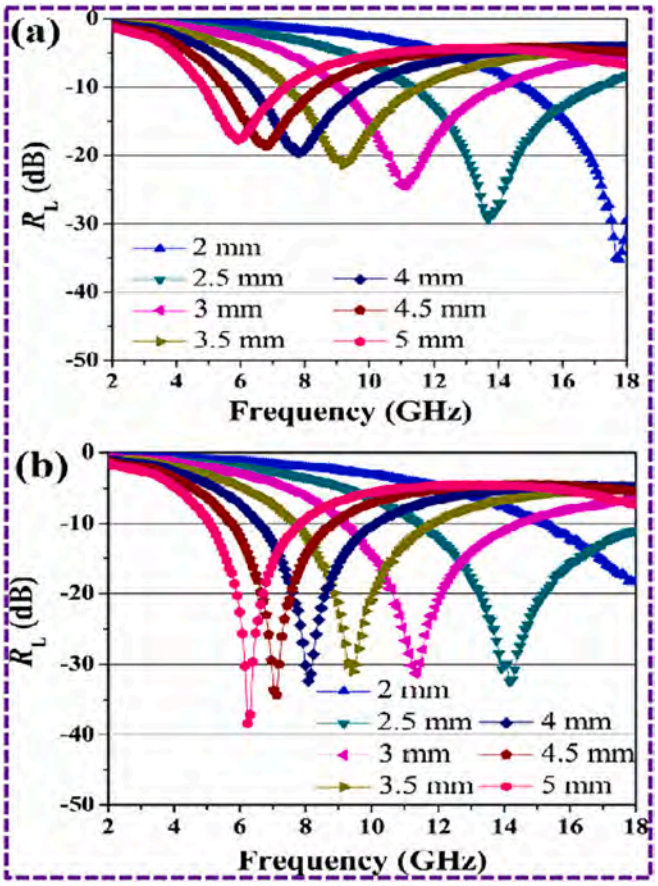

Fig. 21. Reflection losses of the (a) G/Fe_3O_4@Fe ternary nanocomposites and (b) G/Fe_3O_4@Fe/ZnO quaternary nanocomposites with thickness 2–5 mm. Reproduced with permission from ref. [112]. Copyright 2012, ACS Publication.

(5.78 GHz at 2.5 mm) due to its greater frequency range approaching at impedance matching $|Z_{in}/Z_0|$ =1 in the 2–18 GHz. Consequently, it can be said that the S3 exhibited a better electromagnetic wave absorbing performance (broader EAB and stronger RL intensity 20.66 dB) than the S1, S2, and S4, primarily due to the synergistic effect of excellent electromagnetic wave attenuation capacity and superior impedance matching caused by multiple constituents and hierarchical structures.

Ultra-light 3D reduced graphene oxide aerogels embellished with

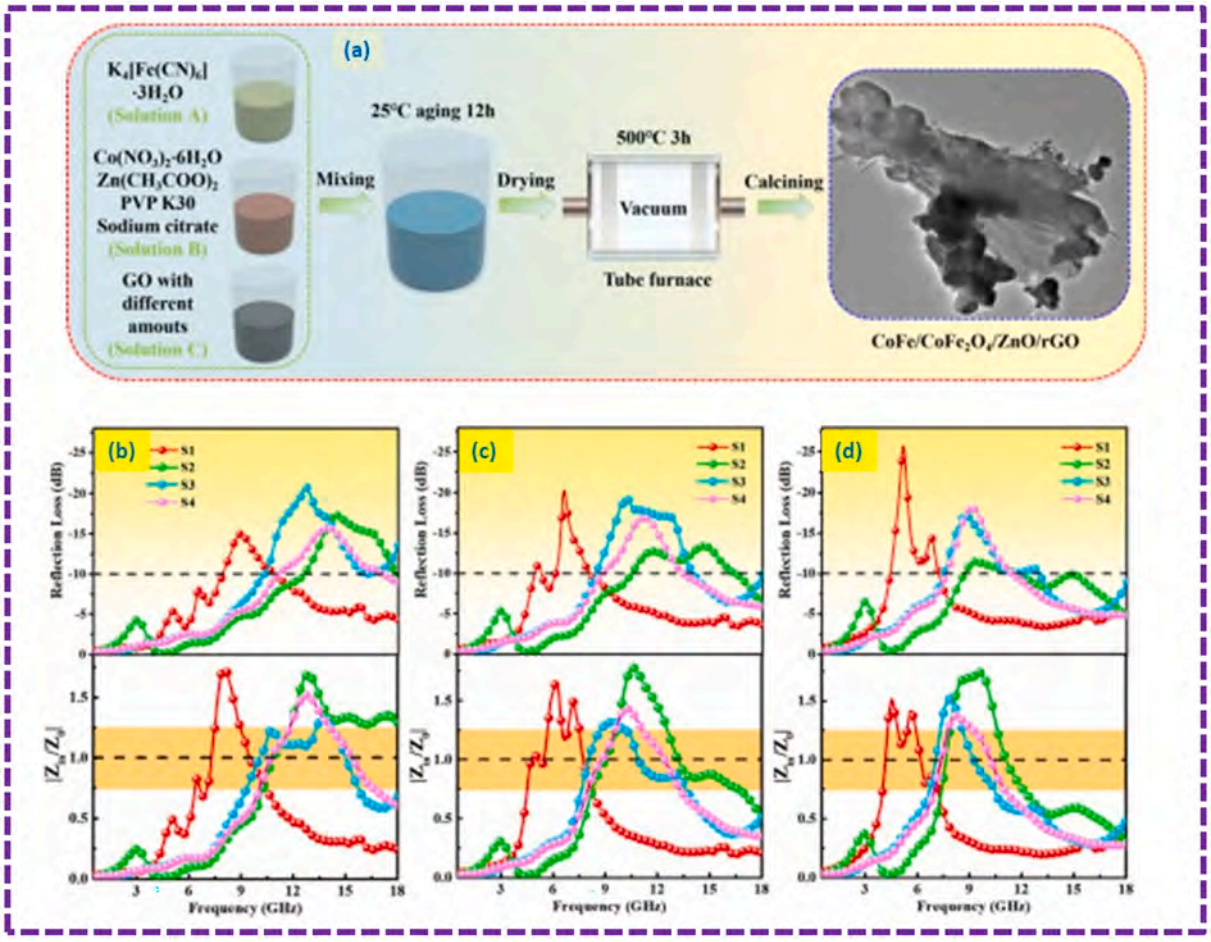

Fig. 22. (a) Schematic illustration for the synthesis of CoFe/$CoFe_2O_4$/ZnO/rGO composites. Reproduced with permission from ref. [113]. Copyright 2023, Elsevier Publication. Impedance matching $|Z_{in}/Z_0|$ and corresponding RL values of samples at 2.5 mm (b), 3.0 mm (c), and 3.5 mm (d). Reproduced with permission from ref. [113]. Copyright 2023, Elsevier Publication.

$CoFe_2O_4$ and ZnO for high electromagnetic interference shielding implementation, was reported by Shivam Gupta et al. [114]. For preparation of aerogel composites, the flash pyrolysis approach was used to prepare cobalt ferrite (CFO) nanoparticles and graphene oxide (GO) was developed by the modified Hummers method (Fig. 23). The graphene aerogel demonstrated total EMI shielding effectiveness of 25.07 dB at a thickness of 5 mm due to its low density, high porosity, and wide surface area. This value was increased to 42.10 dB with the addition of cobalt ferrite nanoparticles. The total EMI shielding effectiveness and power absorption increased to 48.56 dB and 93.655%, respectively, by further integrating ZnO nanorods along with cobalt ferrite nanoparticles into the aerogels.

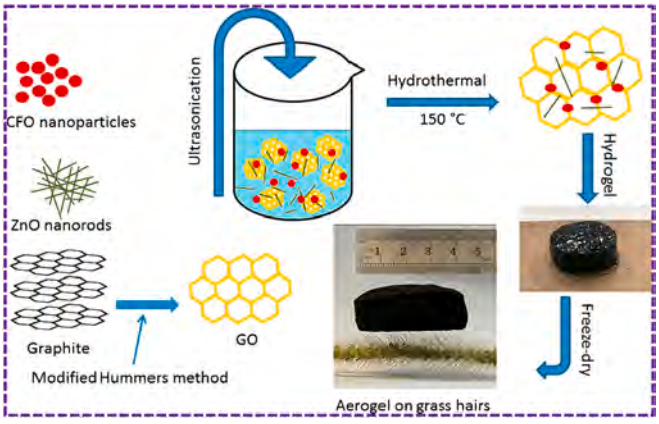

Fig. 23. Schematic representation of the aerogel preparation. Reproduced with permission from ref. [114]. Copyright 2019, Elsevier Publication.

Fei Li et al. [115] reported $ZnFe_2O_4$@ZnO@rGO nanocomposites for enhanced electromagnetic wave absorption. It was possible to create $ZnFe_2O_4$ adorned with ZnO nanoparticles and combine them with reduced graphene oxide (rGO) to create $ZnFe_2O_4$@ZnO@rGO ternary hierarchical nanocomposites. The ZnO crystals formed the ternary nanocomposites by growing on the $ZnFe_2O_4$ nanoparticles' surfaces and wrapping them with rGO nanosheets (Fig. 24). The $ZnFe_2O_4$@ZnO@rGO nanocomposites exhibited reflection loss (RL) -35.2 dB at 12.0 GHz at a 2.0 mm thickness, and the effective absorption bandwidth 3.7 dB (Fig. 24). Controlling the amount of ZnO and rGO in the composites efficiently control their permittivity and permeability, resulting in good impedance matching. The $ZnFe_2O_4$@ZnO@rGO nanocomposites displayed significant wave absorption and wide absorption bandwidth due to the synergistic effect of dielectric loss and magnetic loss.

Wei Wang et al. [116] reported hollow ZnO/$ZnFe_2O_4$ microspheres anchored graphene aerogels as an enhanced electromagnetic wave absorber. By using hydrothermal and lyophilization techniques, hollow ZnO/$ZnFe_2O_4$ microspheres were enclosed and spread over the surface of the reduced graphene aerogel (rGA) (Fig. 25). With a lowest RL of -65.2 dB at 11.3 GHz and a widest EAB range of 9.1 GHz (8.9 GHz–18 GHz) at a mass ratio of 10 wt%, the developed ZnO/$ZnFe_2O_4$/rGA composite displayed exceptional EM absorption capabilities. This outstanding performance was attributed to the excellent synergy

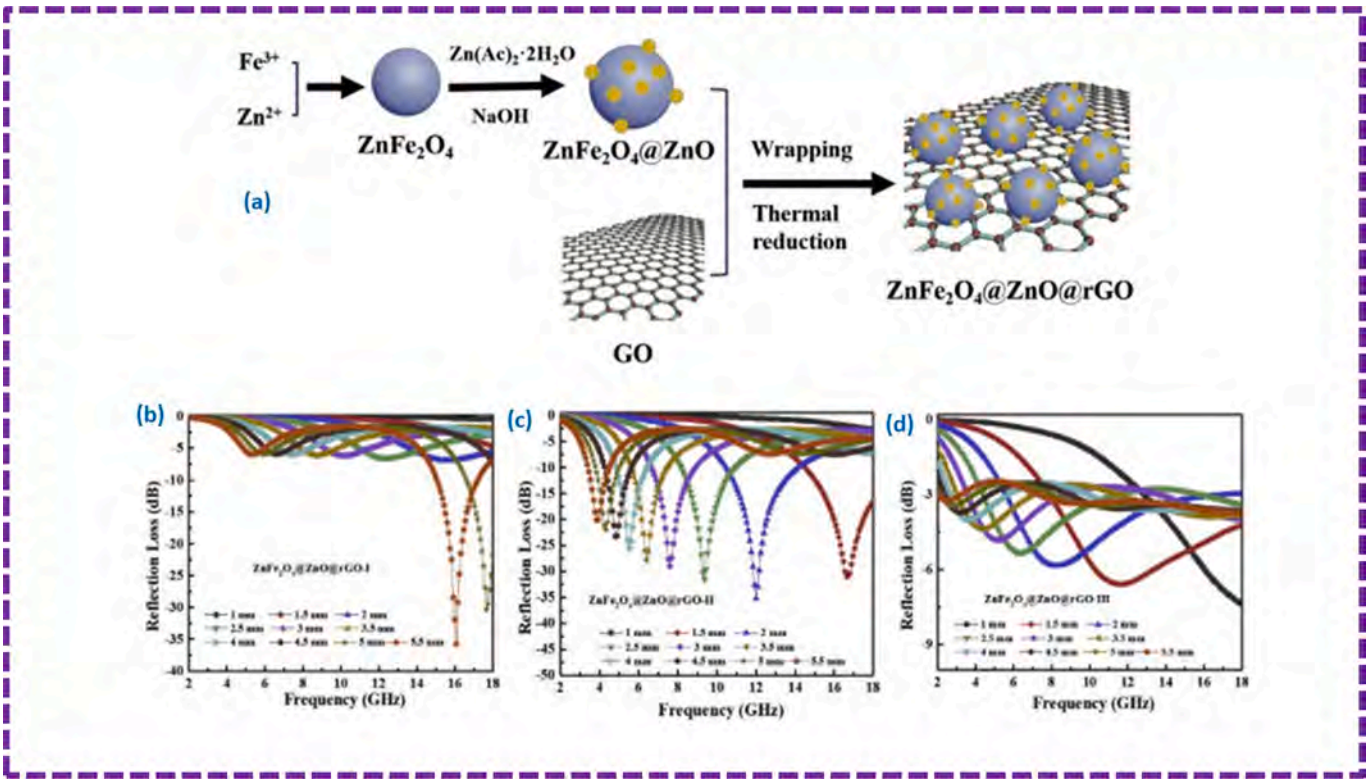

Fig. 24. (a) Schematic illustration for the fabrication process of $ZnFe_2O_4$@ZnO@rGO nanocomposites. Reproduced with permission from ref. [115]. Copyright 2020, Elsevier Publication. RL of $ZnFe_2O_4$@ZnO@rGO with different rGO content (mixed with paraffin, the $ZnFe_2O_4$@ZnO@rGO content was 30 wt%) with a thickness of 1–5.5 mm in 2–18 GHz: (b) $ZnFe_2O_4$@ZnO@rGO-I; (c) $ZnFe_2O_4$@ZnO@rGO-II; (d) $ZnFe_2O_4$@ZnO@rGO-III. Reproduced with permission from ref. [115]. Copyright 2020, Elsevier Publication.

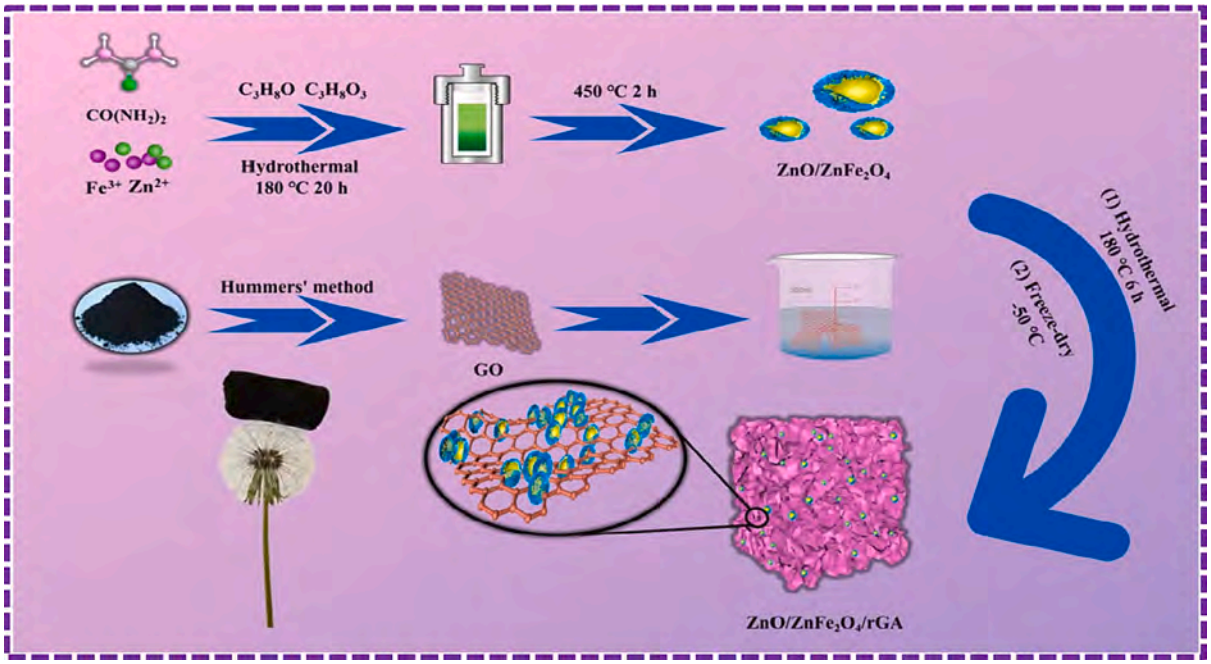

Fig. 25. Schematic illustration of as-obtained ZnO/$ZnFe_2O_4$/rGA composite. Reproduced with permission from ref. [116]. Copyright 2023, Elsevier Publication.

between the ZnO/$ZnFe_2O_4$ hollow microspheres and the rGA backbone, the multiple reflections and scattering brought on by the aerogel's 3D porous structure, the dipole and interface polarization produced by the heterogeneous interface, and the suitable magnetic loss offered by natural and exchange resonances.

Due to their suitable impedance matching and robust attenuation constant, hierarchical composites with both magnetic loss and dielectric loss materials are quite desirable for high-performance microwave absorbers. Yan Wang et al. [117] reported hierarchical $NiFe_2O_4$/ nitrogen-doped graphene(N-GN)/ZnO composite as an efficient electromagnetic

wave absorber. By using an easy hydrothermal process to generate ZnO nanoflowers on magnetically decorated graphene, the hierarchical $NiFe_2O_4$/N-GN/ZnO composite was created. With a modest filler loading of 20 wt% and a thickness of 2.7 mm, the $NiFe_2O_4$/N-GN/ZnO composite exhibited dramatically increased EM absorption capability with RL_{max} of −70.7 dB at 13.5 GHz. It was possible to produce an effective absorption bandwidth of up to 3.5 GHz (11.7–15.2 GHz; RL ≤ −10 dB). Because of good impedance matching and a synergistic effect, the $NiFe_2O_4$/N-GN/ZnO composite (20 wt%) demonstrated higher absorption characteristics when compared to other filler loadings. ZnO nanoflowers help to facilitate multiple scattering and interfacial polarization in voids, which enhances microwave absorption performance (Fig. 26). The microwave absorption property is also significantly influenced by other absorption mechanisms such as electron polarization relaxation, dipole polarization, and defect polarization relaxation processes. $Ni_{1-x}Zn_xFe_2O_4$/$FeNi_3$/ZnO composite powders for electromagnetic wave absorption were described by S. Golchinvafa et al. [118]. A solution combustion approach was used to combine the precursor solutions of $Ni_{1-x}Zn_xFe_2O_4$ and ZnO to in-situ create the composite absorbers with uniform phase distribution. The composite incorporating amorphous ZnO phase demonstrated good microwave absorption capability and exhibited the maximum RL of −41 dB in the X frequency band at a matching thickness of 2.8 mm. In addition, a summary on recent progress on ZnO and spinel ferrite-based nanocomposites for EMI shielding and microwave absorption is tabulated in Table 6.

Table 6
Summary on recent progress on ZnO and spinel ferrite-based nanocomposites for EMI shielding and microwave absorption.

No.	Material	Frequency band	Optimum thickness	RL_{min} /SE_T	Ref.
1.	3D (Fe_3O_4/ZnO)@C double-core@shell porous nano composites	2–18 GHz	2 mm	−40 dB	[109]
2.	Fe_3O_4 nanoparticle-decorated ZnO nanorod-based microflowers	2–18 GHz	2.7 mm	−36.2 dB	[110]
3.	G/Fe_3O_4@Fe/ZnO quaternary nanocomposites	2–18 GHz	5 mm	−38.4 dB	[112]
4.	reduced graphene oxide aerogels embellished with $CoFe_2O_4$ and ZnO	8.2–12.4 GHz	5 mm	48.56 dB	[114]
5.	$ZnFe_2O_4$@ZnO@rGO	2–18 GHz	2 mm	−35.2 dB	[115]
6.	ZnO/$ZnFe_2O_4$/rGA composite	2–18 GHz	3.3 mm	- 65.2 dB	[116]
7.	$NiFe_2O_4$/N-GN/ZnO	2–18 GHz	2.7 mm	−70.7 dB	[117]
8.	$Ni_{1-x}Zn_xFe_2O_4$/$FeNi_3$/ZnO	2–18 GHz	2.8 mm	− 41 dB	[118]

4.7. ZnO and polymer based nanocomposites

Researchers have recently paid a great deal of attention to the coupling of polymers with ZnO semiconductor materials to improve the reflection loss of EM waves. For instance, Leilei Zhang et al. [119] discovered polypyrrole decorated flower- and rod-like ZnO composites with increased microwave absorption performance. By using in-situ polymerization and the hydrothermal technique, ZnO/PPy composites with flower- and rod-like structures were created. The microwave absorption performance of the rod-like ZnO/PPy composites was better than that of the flower-like ZnO/PPy composites. At a thickness of 2.7 mm, the rod-like ZnO/PPy composites exhibited RL_{min} values of −59.7 dB and EAB values of 6.4 GHz. This work suggested that in order to increase the dielectric properties of rod-like ZnO/PPy composites, create multiple reflections of incident electromagnetic waves, and create an interfacial polarization effect, as well as improve the microwave absorption properties of composite materials, PPy must be added, and the composites must be stacked. Xiaoyun Ye et al. [120] reported polypyrrole decorated hollow porous ZnO microspheres for enhanced microwave absorption. The ZnO hollow porous microspheres (ZnO HPM) were made using a hydrothermal technique. PPy was then blended onto the microspheres' surfaces using the in-situ polymerization technique to create ZnO@PPy hollow porous composites (ZnO@PPy HPC). At a thin thickness of 2.2 mm, the ZnO@PPy composites displayed RL_{min} values of - 48.5 dB and 6.2 GHz. The superior electromagnetic wave performance was attributed to the enhanced impedance matching capability, effective multiple loss mechanism, and interfacial polarization.

Ali Olad et al. [121] reported the Epoxy-PPy/Fe_3O_4-ZnO nanocomposite for electromagnetic absorber. The Epoxy-PPy/Fe_3O_4-ZnO nanocomposite with an iron oxide to zinc oxide ratio of 2:1 experienced the highest reflection loss, which was −32.53 dB, at 9.96 GHz. The absorption bandwidth, which covered the frequency range of 8.2–12.4 GHz, was up to 4.2 GHz with a reflection loss of less than −10 dB (90%

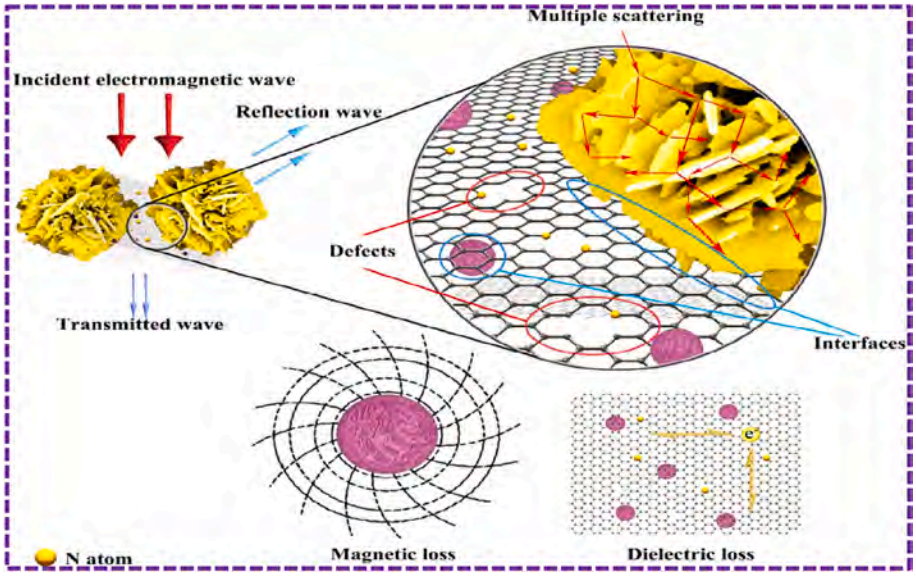

Fig. 26. Schematic illustration of microwave absorption mechanism based on $NiFe_2O_4$/N-GN/ZnO hierarchical composite. Reproduced with permission from ref. [117]. Copyright 2019, Elsevier Publication.

attenuation).

G.P. Abhilash et al. [122] described polymer composites with dielectric $BaTiO_3$ and semiconducting ZnO nanoparticles on rGO layers for electromagnetic wave absorber. Acrylonitrile butadiene styrene (ABS) polymer was combined with the nanofillers rGO-$BaTiO_3$ and rGO-ZnO with multiwall carbon nanotube (MWCNT) to create polymer composites. The weight ratio and shield thickness were also adjusted to manage total shielding effectiveness (SE_T) (Fig. 27). The 10 wt% rGO-$BaTiO_3$ composite showed a SE_T of 40.5 dB in the X-band and a maximum SE_T of 59.8 dB at 11.8 GHz. In the instance of rGO-ZnO composites, 45.1 dB was displayed, and the highest SE_T that was seen 57.9 dB at 9.6 GHz. Multicomponent composites enabled the attenuation of electromagnetic waves. The multicomponent conductive network of rGO sheets and nanoparticles that benefited from impedance matching was synergistically enhanced by the composite films, which demonstrated their excellent compatibility and potential for use in electronics, electromagnetic countermeasures, and stealth materials. A gradient EMI composite foam of MXene/Ag@ZnO/WPU/Melamine was proposed by Tongcheng Zuo et al. [123]. It was made using a straightforward unidirectional evaporation technique in conjunction with a vacuum-drying technique. The as-prepared M_2A_3F composite material with an ultra-low volume ratio (2.72% MXene and 4.25% Ag), exhibited a low reflectivity coefficient of 0.1423, and a high EMI SE of 39.90 dB under the influence of "absorb-reflect-reabsorb." Further, in order to protect against electromagnetic energy, Palash Das et al. [124] created a multifunctional, high-strength elastomeric nanocomposite that is extremely flexible, self-repairing, recyclable, and has great temperature management characteristics. The developed ZnO-XNBR/RGO nanocomposites exhibited an EMI SE of −34.2 dB in the X-band (8.2–12.4 GHz).

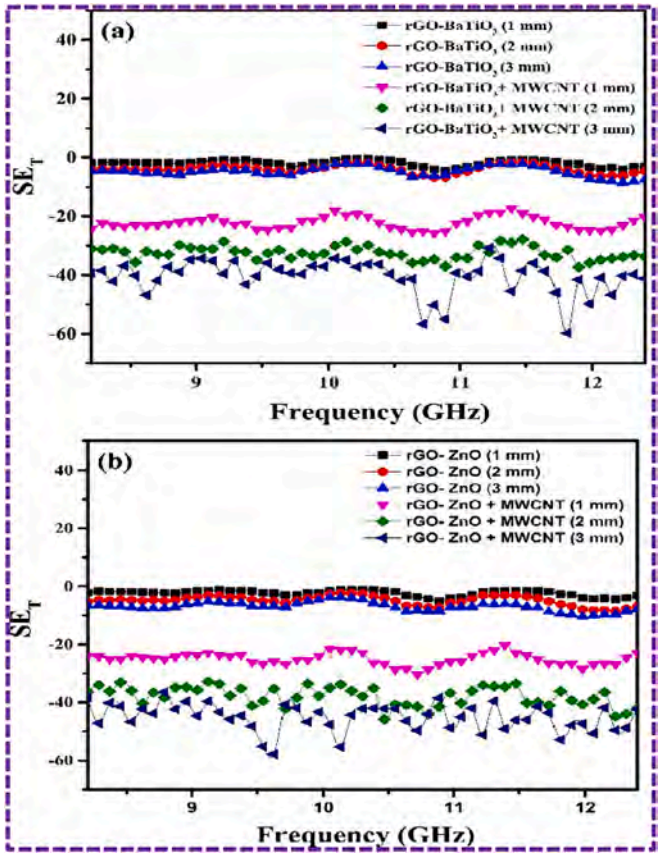

Fig. 27. Total shielding (SE_T) of (a) rGO-$BaTiO_3$ and (b) rGO-ZnO composites. Reproduced with permission from ref. [122]. Copyright 2023, Elsevier Publication.

In addition, a summary on recent progress on ZnO and polymer-based nanocomposites for EMI shielding and microwave absorption is tabulated in Table 7.

4.8. ZnO and textile based nanocomposites

In a variety of recent applications, wearable functional materials and gadgets have drawn a lot of attention. Because cotton fabrics have a long history of use as clothing materials, they are regarded as the greatest possibility for wearable electronics. However, because cotton fabrics are naturally non-conducting and nearly transparent to EM waves, additional processing is necessary to obtain the needed qualities. For instance, Shivam Gupta et al. [125] reported a wearable electrically conductive cotton textile with reduced graphene oxide/zinc oxide coating for strong microwave absorption. The cotton fabrics were first evenly coated with ZnO nanoparticles using a straightforward and affordable sol-gel approach, and then coated with rGO using a quick spraying and drying procedure, followed by thermal annealing (Fig. 28). The core-shell structure of the rGO/ZnO coated cotton, in which the uniform layers of ZnO and rGO performed the roles of the double-layered shell and the annealed cotton served as the core, was discovered to be promising for the absorption dominated wearable EMI shielding. The interactions between the highly conductive rGO nanosheets, highly dielectric ZnO nanoparticles, and interconnected annealed cotton fiber networks were extremely advantageous for absorption-dominant EMI shielding. The highest total EMI shielding effectiveness of 99.999% (54.7 dB), which is shared by 17.783% of reflection and 82.216% of absorption, is achieved by the as-prepared rGO/ZnO coated cotton (ZnO + 7 wt% rGO).

For improved microwave absorption, Shijun Wang et al. [126] presented hierarchical $Ti_3C_2T_x$ MXene/Ni Chain/ZnO array hybrid nanostructures on cotton fabric. Using simple dip-coating and hydrothermal techniques, hierarchical $Ti_3C_2T_x$ MXene/Ni chain/ZnO array hybrid nanostructures on cotton fabric were created (Fig. 29). Intensely coated cotton fiber surfaces with conductive MXene nanosheets can give the cotton fabric substrate exceptional dielectric characteristics. The ordered ZnO array construction has a large amount of empty space and a high aspect ratio, which can produce different polarization and broaden the EM wave propagation routes. In addition to adding magnetic loss to textile-based microwave absorber materials, the magnetic Ni chains incorporated into ZnO arrays can further enhance impedance matching. By adjusting the quantity of Ni chains that are dip-coated, the electromagnetic properties of the fabric can be further tuned to enhance electromagnetic wave absorption performance. The developed fabric's effective absorption band can cover the entire X-band with only a 2.2 mm thickness, and its minimum RL value can reach −35.1 dB at 8.3 GHz with a thickness of 2.8 mm. MXenes, Ni chains, and ZnO arrays all have synergistic microwave absorption mechanisms that result from dielectric loss, magnetic loss, multiple reflection, and scattering (Fig. 29).

Table 7
Summary on recent progress on ZnO and polymer-based nanocomposites for EMI shielding and microwave absorption.

No.	Material	Frequency band	Optimum thickness	RL_{min} /SE_T	Ref.
1.	rod-like ZnO/PPy composites	2–18 GHz	2.7 mm	−59.7 dB	[119]
2.	ZnO@PPy composites	2–18 GHz	2.2 mm	−48.5 dB	[120]
3.	Epoxy-PPy/Fe_3O_4-ZnO	8.2–12.4 GHz	–	−32.53 dB	[121]
4.	rGO-$BaTiO_3$/MWCNT	8.2–12.4 GHz	3 mm	59.8 dB	[122]
5.	MXene/Ag@ZnO/WPU/Melamine	8.2–12.4 GHz	4 mm	39.90 dB	[123]
6.	ZnO-XNBR/RGO	8.2–12.4 GHz	1 mm	−34.2 dB	[124]

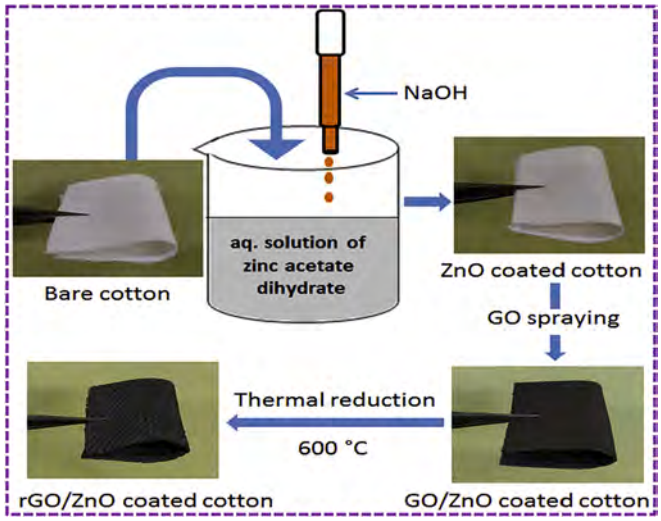

Fig. 28. Schematic representation of the preparation process for rGO/ZnO coated cotton. Reproduced with permission from ref. [125]. Copyright 2020, Elsevier Publication.

Therefore, the synergistic impacts of the aforementioned parameters, which considerably increased the EM wave attenuation capacity and optimized the impedance matching, were responsible for the produced fabric's superior microwave absorption performance. With potential uses in flexible and wearable functional electronics, this research group's work offers insight into the logical design of textile-based microwave absorption materials.

Xiaopeng Han et al. [127] reported the flexible hierarchical carbon cloth-based film for efficient microwave absorption. This study team created brand-new integrated dielectric hybrid composites with ZnO arrays embellished on a stretchable carbon cloth (CC) matrix with customizable structure. Excellent RL values of - 47.3 dB at 2.5 mm and the widest effective absorption band of 4.0 GHz in the whole X band were demonstrated by the optimized CC@ZnO film. By coating cotton fabric in a synergistic manner with reduced graphene oxide-magnetic ferrite nanoparticles (RGO-MF) and vertically aligned zinc oxide nanorods (ZnO NRs), Shivam Gupta et al. [128] presented a novel method to improve EMI shielding. As a result of the exceptional conductivity of RGO sheets, the strong magnetism of MF nanoparticles, the remarkable dielectric properties of ZnO NRs, and the enhanced core-shell structure of the cotton fabric containing these materials, the RGO-MF/ZnO NRs coated cotton exhibited a high total EMI shielding effectiveness of ~55 dB, reflection loss of 6.8 dB, and an absorption coefficient of 74.5%. In addition, a summary on recent progress on ZnO and textile-based nanocomposites for EMI shielding and microwave absorption is tabulated in Table 8.

5. Conclusion and future prospects

In this review article, we reviewed recent advances on electromagnetic wave shielding and microwave absorption of nanocomposites of ZnO semiconductors, including preparation techniques; impact of addition of graphene, carbon nanotube, MXene, spinel ferrite magnetic nanoparticles, polymer and textile on the electromagnetic wave absorption performances of ZnO semiconductor material. The electromagnetic wave absorption properties, including minimum RL values and effective absorption bandwidth of developed nanocomposites of ZnO semiconductors are summarized. There is a detailed description of the theoretical links between the created ZnO semiconductor nanocomposites' magnetic, dielectric, and conductive properties and their EMI shielding properties. ZnO semiconductor materials' porous nanoarchitectures are useful for producing numerous reflections, which enhance EM wave absorption. Due to interfacial polarization and magnetic losses, the addition of magnetic nanoparticles with advanced magnetic properties enhances the EMI shielding capabilities of ZnO semiconductor materials.

Table 8
Summary on recent progress on ZnO and textile-based nanocomposites for EMI shielding and microwave absorption.

No.	Material	Frequency band	Optimum thickness	RL_{min} /SE_T	Ref.
1.	rGO/ZnO coated cotton	8.2–12.4 GHz	–	54.7 dB	[125]
2.	Ti3C2Tx MXene/Ni Chain/ZnO / cotton fabric	8.2–12.4 GHz	2.8 mm	−35.1 dB	[126]
3.	carbon cloth @ZnO film	2–18 GHz	2.5 mm	- 47.3 dB	[127]
4.	RGO-MF/ZnO NRs coated carbonized cotton	2–18 GHz	–	~55 dB	[128]

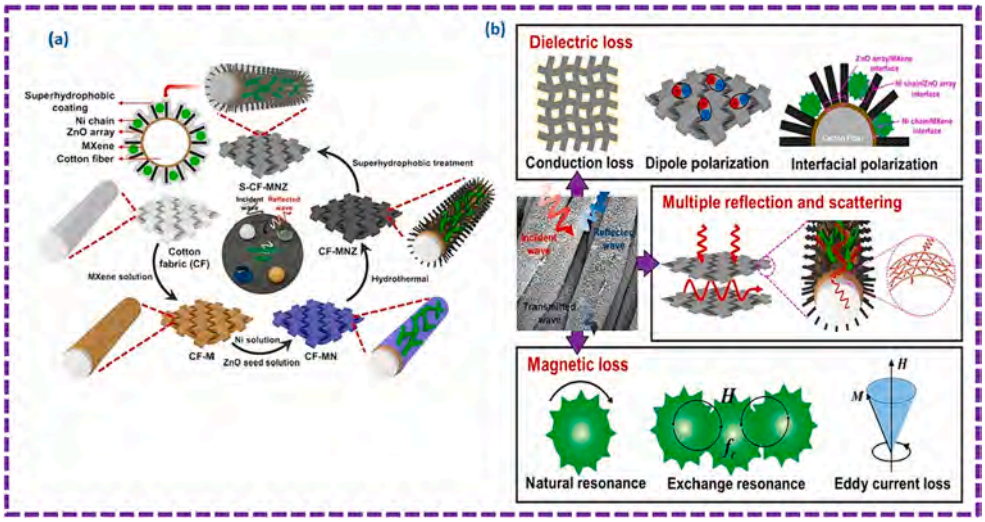

Fig. 29. (a) Schematic illustration of preparation process of MXene/Ni chain/ZnO array cotton fabrics. Reproduced with permission from ref. [126]. Copyright 2020, ACS Publication. (b) Schematic illustration of MA mechanisms of MXene/Ni chain/ZnO array cotton fabrics. Reproduced with permission from ref. [126]. Copyright 2020, ACS Publication.

It is clear that there are still a number of difficulties associated with using ZnO semiconductors as the principal components for EMI shielding, despite the significant advancements that have already been made in the field. The most urgent problems and some potential solutions are as follows:

1. The researchers still need to have a better understanding of the idea of impedance matching and its function in the context of EMI shielding and microwave absorption for ZnO semiconductor nanocomposite.
2. It is still challenging to develop effective EMI shielding nanocomposite materials using ZnO semiconductor having specific nanostructures, and more study is required.
3. ZnO semiconductor materials' electrical conductivity is improved by doping. As a result, it is anticipated that adding appropriate foreign elements will enhance the EMI shielding capabilities of ZnO semiconductor-based nanocomposites.
4. The majority of the research on EMI shielding and microwave absorbers is conducted in laboratories. However, in addition to conducting fundamental research, efforts should be made to create items that are near to being used in real-world situations and being produced in large quantities.
5. By transforming electromagnetic radiation into heat, EMI shielding, and microwave absorbers can provide electromagnetic protection. Can the heat produced, nevertheless, be put to use? Thermoelectric conversion theories are evolving, but there are only theoretical studies, no relevant experimental data, and no usable equipment.

These obstacles must be overcome in order to produce ZnO semiconductor-based EMI shielding and microwave absorber nanocomposites that are economically viable. On this goal should be the focus of future research directions.

CRediT authorship contribution statement

Raghvendra Singh Yadav: Conceptualization, Formal analysis, Funding acquisition, Investigation, Methodology, Supervision, Validation, Visualization, Writing – original draft, Writing – review & editing. **Ivo Kuřitka:** Funding acquisition, Project administration, Visualization.

Declaration of competing interest

The authors declare that they have no known competing financial interests or personal relationships that could have appeared to influence the work reported in this paper.

Data availability

No data was used for the research described in the article.

Acknowledgement

This work was supported by Ministry of Education, Youth, and Sports of the Czech Republic- DKRVO (RP/CPS/2022/007) at the Centre of Polymer Systems, Tomas Bata University in Zlin, Czech Republic.

References

[1] Wang H-Y, Sun X-B, Yang S-H, Zhao P-Y, Zhang X-J, Wang G-S, et al. 3D ultralight hollow NiCo compound@MXene composites for tunable and high-efficient microwave absorption. Nano-Micro Lett 2021;13:206.
[2] Jiang X, Zhao Z, Zhou S, Zou H, Liu P. Anisotropic and lightweight carbon/graphene composite aerogels for efficient thermal insulation and electromagnetic interference shielding. ACS Appl Mater Interfaces 2022;14:45844–52.
[3] Pan Y, Dai M, Guo Q, Yin D, Hu S, Hu N, et al. Construction of sandwich-structured Cu-Ni wood-based composites for electromagnetic interference shieldin. Chem Eng J 2023;471:144301.
[4] Sankaran S, Deshmukh K, Ahamed MB, Khadheer Pasha SK. Recent advances in electromagnetic interference shielding properties of metal and carbon filler reinforced flexible polymer composites: a review. Compos Part A 2018;114:49–71.
[5] Kumar R, Sahoo S, Joanni E, Singh RK, Tan WK, Moshkalev SA, et al. Heteroatom doping of 2D graphene materials for electromagnetic interference shielding: a review of recent progress. Crit Rev Solid State Mater Sci 2022;47(4):570–619. https://doi.org/10.1080/10408436.2021.1965954.
[6] Gupta S, Tai N-H. Carbon materials and their composites for electromagnetic interference shielding effectiveness in X-band. Carbon 2019;152:159–87.
[7] Kumar R, Sahoo S, Joanni E. Composites based on layered materials for absorption of microwaves and electromagnetic shielding. Carbon 2023;211:118072.
[8] Abdalla I, Cai J, Lu W, Yu J, Li Z, Ding B. Recent progress on electromagnetic wave absorption materials enabled by electrospun carbon nanofibers. Carbon 2023;213:118300.
[9] Yadav RS, Kuritka I, Vilcakova J. Advanced spinel ferrite nanocomposites for electromagnetic interference shielding applications. Elsevier; 2021.
[10] Yadav RS, Anju Kuritka I. Spinel ferrite and MXene-based magnetic novel nanocomposites: an innovative high-performance electromagnetic interference shielding and microwave absorber. Crit Rev Solid State Mater Sci 2023;48(4):441–79.
[11] Yadav RS, Kuritka I. Recent developments on nanocomposites based on spinel ferrite and carbon nanotubes for applications in electromagnetic interference shielding and microwave absorption. Crit Rev Solid State Mater Sci 2023. https://doi.org/10.1080/10408436.2023.2214577.
[12] Zheng S, Wang Y, Wang X, Lu H. Research progress on high-performance electromagnetic interference shielding materials with well-organized multilayered structures. Mater Today Phys 2024;40:101330.
[13] Xiong X, Zhang H, Lv H, Yang L, Liang G, Zhang J, et al. Recent progress in carbon-based materials and loss mechanisms for electromagnetic wave absorption. Carbon 2024;219:118834.
[14] Wei H, Li W, Bachagha K. Component optimization and microstructure design of carbon nanotube-based microwave absorbing materials: a review. Carbon 2024;217:118651.
[15] Jiang Z, Liu B, Yu L, Tong Y, Yan M, Zhang R, et al. Research progresses in preparation methods and applications of zinc oxide nanoparticles. J Alloys Compd 2023;956:170316.
[16] Peksu E, Coskun A, Karaagac H. Recent progress in solar cells based on one dimensional ZnO nanostructures. Nanotechnology 2023;34:352003 (38pp).
[17] Singh P, Singh RK, Kumar R. Journey of ZnO quantum dots from undoped to rare-earth and transition metal-doped and their applications. RSC Adv 2021;11:2512.
[18] Singh S, Thiyagarajan P, Kant KM, Anita D, Rama STN, Tiwari B, et al. Structure, microstructure and physical properties of ZnO based materials in various forms: bulk, thin film and nano. J Phys D Appl Phys 2007;40:6312–27.
[19] Jeong WJ, Kim SK, Park GC. Preparation and characteristic of ZnO thin film with high and low resistivity for an application of solar cell. Thin Solid Films 2006;506-507:180–3.
[20] Brasiunas B, Popov A, Lisyte V, Kausaite-Minkstimiene A, Ramanaviciene A. ZnO nanostructures: a promising frontier in immunosensor development. Biosens Bioelectron 2024;246:115848.
[21] Kumar R, Umar A, Kumar G, Nalwa HS. Antimicrobial properties of ZnO nanomaterials: a review. Ceram Int 2017;43 (3940–396).
[22] Wang G-S, Wu Y-Y, Zhang X-J, Li Y, Guo L, Cao M-S. Controllable synthesis of uniform ZnO nanorods and their enhanced dielectric and absorption properties. J Mater Chem A 2014;2:8644.
[23] Song C, Yin X, Han M, Li X, Hou Z, Zhang L, et al. Three-dimensional reduced graphene oxide foam modified with ZnO nanowires for enhanced microwave absorption properties. Carbon 2017;116:50–8.
[24] He G, Duan Y, Pang H, Hu J. Superior microwave absorption based on ZnO capped MnO_2 nanostructures. Adv Mater Interfaces 2020;7:2000407.
[25] Liu X, Lu X, Guan H, Liu X, Wang Y, Zhao D, et al. Controllable synthesis of flower-like ZnO modified by CuO nanoparticles/N-RGO composites for efficient microwave absorption properties. Ceram Int 2022;48:6948–55.
[26] Green M, Chen X. Recent progress of nanomaterials for microwave absorption. J Mater 2019;5(4):503–41. https://doi.org/10.1016/j.jmat.2019.07.003.
[27] Li L, Chen Z, Pan F, Guo H, Wang X, Cheng J, et al. Electrospinning technology on one dimensional microwave absorbers: fundamentals, current progress, and perspectives. Chem Eng J 2023;470:144236.
[28] Guan H, Wang Q, Wu X, Pang J, Jiang Z, Chen G, et al. Biomass derived porous carbon (BPC) and their composites as lightweight and efficient microwave absorption materials. Compos Part B Eng 2021;207:108562. https://doi.org/10.1016/j.compositesb.2020.108562.
[29] Yadav RS, Kuřitka I, Vilcakova J, Skoda D, Urbánek P, Machovsky M, et al. Lightweight $NiFe_2O_4$-reduced graphene oxide-elastomer nanocomposite flexible sheet for electromagnetic interference shielding application. Compos Part B 2019;166:95–111.
[30] Meng F, Wang H, Huang F, Guo Y, Wang Z, Hui D, et al. Graphene-based microwave absorbing composites: a review and prospective. Compos Part B Eng 2018;137:260–77. https://doi.org/10.1016/j.compositesb.2017.11.023.
[31] Song W-L, Zhang K-L, Chen M, Hou Z-L, Chen H, Yuan X, et al. A universal permittivity-attenuation evaluation diagram for accelerating design of dielectric-based microwave absorption materials: a case of graphene-based composites. Carbon 2017;118:86–97. https://doi.org/10.1016/j. carbon.2017.03.016.

[32] Zhao H-B, Cheng J-B, Zhu J-Y, Wang Y-Z. Ultralight CoNi/rGO aerogels toward excellent microwave absorption at ultrathin thickness. J Mater Chem C 2019;7(2):441–8. https://doi.org/10.1039/c8tc05239e.

[33] Wang W, Zhang H, Zhao Y, Wang J, Zhao H, Li P, et al. A novel MOF-drived self-decomposition strategy for CoO@N/C-Co/Ni-$NiCo_2O_4$ multi-heterostructure composite as high-performance electromagnetic wave absorbing materials. Chem Eng J 2021;426:131667. https://doi.org/10.1016/j.cej.2021.131667.

[34] Zhang X, Li Y, Liu R, Rao Y, Rong H, Qin G. High-magnetization FeCo nanochains with ultrathin interfacial gaps for broadband electromagnetic wave absorption at gigahertz. ACS Appl Mater Interfaces 2016;8:3494–8. https://doi.org/10.1021/acsami.5b12203.

[35] Guan H, Wang Q, Wu X, Pang J, Jiang Z, Chen G, et al. Biomass derived porous carbon (BPC) and their composites as lightweight and efficient microwave absorption materials. Compos Part B 2021;207:108562.

[36] Guan H, Wang Q, Wu X, Pang J, Jiang Z, Chen G, et al. Biomass derived porous carbon (BPC) and their composites as lightweight and efficient microwave absorption materials. Compos Part B Eng 2021;207:108562. https://doi.org/10.1016/j.compositesb.2020.108562.

[37] Yang Y, Xia L, Zhang T, Shi B, Huang L, Zhong B, et al. Fe_3O_4@LAS/RGO composites with a multiple transmission absorption mechanism and enhanced electromagnetic wave absorption performance. Chem Eng J 2018;352:510–8. https://doi.org/10.1016/j.cej.2018.07.064.

[38] Lin Y, Dai J, Yang H, Wang L, Wang F. Graphene multilayered sheets assembled by porous $Bi_2Fe_4O_9$ microspheres and the excellent electromagnetic wave absorption properties. Chem Eng J 2018;334:1740–8. https://doi.org/10.1016/j.cej.2017.11.150.

[39] Cheng Y, Seow JZY, Zhao H, Xu ZJ, Ji G. A flexible and lightweight biomass-reinforced microwave absorber. Nanomicro Lett 2020;12(1):125. https://doi.org/10.1007/s40820-020-00461-x.

[40] Miao P, Yu Z, Chen W, Zhou R, Zhao W, Chen K-J, et al. Synergetic dielectric and magnetic losses of a core-shell Co/MnO/C nanocomplex toward highly efficient microwave absorption. Inorg Chem 2022;61:1787–96.

[41] Wang B, Wu Q, Fu Y, Liu T. A review on carbon/magnetic metal composites for microwave absorption. J Mater Sci Technol 2021;86:91–109. https://doi.org/10.1016/j.jmst.2020.12.078.

[42] Liu Y, Cui T, Wu T, Li Y, Tong G. Excellent microwave-absorbing properties of elliptical Fe_3O_4 nanorings made by a rapid microwave-assisted hydrothermal approach. Nanotechnology 2016;27(16):165707. https://doi.org/10.1088/0957-4484/27/16/165707.

[43] Liang X, Man Z, Quan B, Zheng J, Gu W, Zhang Z, et al. Environment-stable Co_xNi_y encapsulation in stacked porous carbon nanosheets for enhanced microwave absorption. Nanomicro Lett 2020;12(1):102. https://doi.org/10.1007/s40820-020-00432-2.

[44] Shu R, Wu Y, Li Z, Zhang J, Wan Z, Liu Y, et al. Facile synthesis of cobalt zinc ferrite microspheres decorated nitrogen-doped multi-walled carbon nanotubes hybrid composites with excellent microwave absorption in the X-band. Compos Sci Technol 2019;184:107839. https://doi.org/10.1016/j.compscitech.2019.107839.

[45] Lv H, Wu C, Qin F, Peng H, Yan M. Extra-wide bandwidth via complementary exchange resonance and dielectric polarization of sandwiched FeNi@SnO nanosheets for electromagnetic wave absorption. J Mater Sci Technol 2021;90:1–8. https://doi.org/10.1016/j.jmst.2020.12.083.

[46] Liang J, Chen J, Shen H, Hu K, Zhao B, Kong J. Hollow porous bowl-like nitrogen-doped cobalt/carbon nanocomposites with enhanced electromagnetic wave absorption. Chem Mater 2021;33:1789–98.

[47] Miao P, Qu N, Chen W, Wang T, Zhao W, Kong J. A two-dimensional semiconductive Cu-S metal-organic framework for broadband microwave absorption. Chem Eng J 2023;454:140445.

[48] Bao S, Zhang M, Jiang Z, Xie Z, Zheng L. Advances in microwave absorbing materials with broad-bandwidth response. Nano Res 2023. https://doi.org/10.1007/s12274-023-5654-6.

[49] Xiao J, Qi X, Gong X, et al. Defect and interface engineering in core@shell structure hollow carbon@MoS_2 nanocomposites for boosted microwave absorption performance. Nano Res 2022;15:7778–87. https://doi.org/10.1007/s12274-022-4625-7.

[50] Sushmita K, Madras G, Bose S. Polymer nanocomposites containing semiconductors as advanced materials for EMI shielding. ACS Omega 2020;5:4705–18.

[51] Liu J, Wei X, Gao L, Tao J, Xu L, Peng G, et al. An overview of C-SiC microwave absorption composites serving in harsh environments. J Eur Ceram Soc 2023;43:1237–54.

[52] Wang X, Xing X, Zhu H, Li J, Liu T. State of the art and prospects of Fe_3O_4/carbon microwave absorbing composites from the dimension and structure perspective. Adv Colloid Interface Sci 2023;318:102960.

[53] Ding C, Shao C, Wu S, Ma Y, Liu Y, Ma S, et al. A review of 1D carbon-based materials assembly design for lightweight microwave absorption. Carbon 2023;213:118279.

[54] Guo R, Zheng Q, Wang L, Fan Y, Jiang W. Porous N-doped Ni@SiO_2/graphene network: three-dimensional hierarchical architecture for strong and broad electromagnetic wave absorption. J Mater Sci Technol 2022;106:108–17.

[55] Ma M, Liao Z, Su X, Zheng Q, Liu Y, Wang Y, et al. Magnetic CoNi alloy particles embedded N-doped carbon fibers with polypyrrole for excellent electromagnetic wave absorption. J Colloid Interface Sci 2022;608:2203–12.

[56] Jiang B, Qi C, Yang H, Wu X, Yang W, Zhang C, et al. Recent advances of carbon-based electromagnetic wave absorption materials facing the actual situations. Carbon 2023;208:390–409.

[57] Kumar R, Sahoo S, Joanni E. Composites based on layered materials for absorption of microwaves and electromagnetic shielding. Carbon 2023;211:118072.

[58] Sankaran S, Deshmukh K, Ahamed MB, Pasha SKK. Recent advances in electromagnetic interference shielding properties of metal and carbon filler reinforced flexible polymer composites: a review. Compos Part A 2018;114:49–71.

[59] Nan Z, Wei W, Lin Z, Chang J, Hao Y. Flexible nanocomposite conductors for electromagnetic interference shielding. Nano-Micro Lett 2023;15:172.

[60] Kumar R, Kumari S, Dhakate SR. Nickel nanoparticles embedded in carbon foam for improving electromagnetic shielding effectiveness. Appl Nano sci 2015;5(5):553–61.

[61] Omana L, Chandran A, John RE, Wilson R, George KC, Unnikrishnan NV, et al. Recent advances in polymer nanocomposites for electromagnetic interference shielding: a review. ACS Omega 2022;7:25921–47.

[62] Chen Y, Yang Y, Xiong Y, Zhang L, Xu W, Duan G, et al. Porous aerogel and sponge composites: assisted by novel nanomaterials for electromagnetic interference shielding. Nano Today 2021;38:101204.

[63] Iqbal A, Hassan T, Gao Z, Shahzad F, Koo CM. MXene-incorporated 1D/2D nano-carbons for electromagnetic shielding: a review. Carbon 2023;203:542–60.

[64] Cai M, Shui A, Wang X, He C, Qian J, Du B. A facile fabrication and high-performance electromagnetic microwave absorption of ZnO nanoparticles. J Alloys Compd 2020;842:155638.

[65] Zhuo R, Wang Y, Yan D, Li S, Liu Y, Wang F. One-step synthesis and excellent microwave absorption of hierarchical tree-like ZnO nanostructures. Mater Lett 2014;117:34–6.

[66] Zhuo RF, Qiao L, Feng HT, Chen JT, Yan D, Wu ZG, et al. Microwave absorption properties and the isotropic antenna mechanism of ZnO nanotrees. J Appl Phys 2008;104:094101.

[67] Li H, Huang Y, Sun G, Yan X, Yang Y, Wang J, et al. Directed growth and microwave absorption property of crossed ZnO netlike micro-/nanostructures. J Phys Chem C 2010;114:10088–91.

[68] Ren Y, Yang L, Wang L, Xu T, Wu G, Wu H. Facile synthesis, photoluminescence properties and microwave absorption enhancement of porous and hollow ZnO spheres. Powder Technol 2015;281:20–7.

[69] Zhao B, Shao G, Fan B, Xie Y, Sun B, Zhang R. Preparation and microwave absorption of porous hollow ZnO by CO2 soft-template. Adv Powder Technol 2014;25:1761–6.

[70] Sun D, Zou Q, Wang Y, Wang Y, Jiang W, Li F. Controllable synthesis of porous Fe_3O_4@ZnO sphere decorated graphene for extraordinary electromagnetic wave absorption. Nanoscale 2014;6(12):6557–62.

[71] Sun D, Zou Q, Wang Y, Wang Y, Jiang W, Li F. Controllable synthesis of porous Fe_3O_4@ZnO sphere decorated graphene for extraordinary electromagnetic wave absorption. Nanoscale 2014;6(12):6557–62.

[72] Feng W, Wang Y, Chen J, Wang L, Guo L, Ouyang J, et al. Reduced graphene oxide decorated with in-situ growing ZnO nanocrystals: facile synthesis and enhanced microwave absorption properties. Carbon 2016;108:52–60.

[73] Wang X, Yu M, Zhang W, Zhang B, Dong L. Synthesis and microwave absorption properties of graphene/nickel composite materials. Appl Phys A Mater Sci Process 2014;118(3):1053–8.

[74] Singh AK, Kumar A, Srivastava A, Yadav AN, Haldar K, Gupta V, et al. Lightweight reduced graphene oxide-ZnO nanocomposite for enhanced dielectric loss and excellent electromagnetic interference shielding. Compos Part B 2019;172:234–42.

[75] Bao S, Hou T, Tan Q, Kong X, Cao H, He M, et al. Immobilization of zinc oxide nanoparticles on graphene sheets for lithium-ion storage and electromagnetic microwave absorption. Mater Chem Phys 2020;245:122766.

[76] He J-Z, Zeng Q-C, Sun X, Shu J-C, Wang X-X, Cao M-S. Axiolitic ZnO rods wrapped with reduced graphene oxide: fabrication, microstructure and highly efficient microwave absorption. Mater Lett 2019;241:14–7.

[77] Zhang L, Zhang X, Zhang G, Zhang Z, Liu S, Li P, et al. Investigation on the optimization, design and microwave absorption properties of reduced graphene oxide/tetrapod-like ZnO composites. RSC Adv 2015;5:10197.

[78] Liu WW, Li H, Zeng QP, Duan HN, Guo YP, Liu XF, et al. Fabrication of ultralight three-dimensional graphene networks with strong electromagnetic wave absorption properties. J Mater Chem A 2015;3:3739–47.

[79] Yang S, Guo X, Chen P, Xu D-W, Qiu H-F, Zhu X-Y. Two-step synthesis of self-assembled 3D graphene/shuttle-shaped zinc oxide (ZnO) nanocomposites for high-performance microwave absorption. J Alloys Compd 2019;797:1310–9.

[80] Song C, Yin X, Han M, Li X, Hou Z, Zhang L, et al. Three-dimensional reduced graphene oxide foam modified with ZnO nanowires for enhanced microwave absorption properties. Carbon 2017;116:50–8.

[81] Akram MY, Hameed MU, Akhtar N, Ali S, Maitlo I, Zhu X, et al. Synthesis of high performance Ni3C-Ni decorated thermally expanded reduced graphene oxide (TErGO/Ni3C-Ni) nanocomposite: a stable catalyst for reduction of Cr(VI) and organic dyes. J Hazard Mater 2019;366:723–31.

[82] Feng W, Wang Y, Chen J, Wang L, Guo L, Ouyang J, et al. Reduced graphene oxide decorated with in-situ growing ZnO nanocrystals: facile synthesis and enhanced microwave absorption properties. Carbon 2016;108:52–60.

[83] Wang C, Han X, Xu P, Zhang X, Du Y, Hu S, et al. The electromagnetic property of chemically reduced graphene oxide and its application as microwave absorbing material. Appl Phys Lett 2011;98:72906.

[84] Liu X, Zhang F, Lu X, Sun M, Liu X, Yu Z, et al. Simple preparation and microwave absorption of TERGO/ZnO porous composites. Mater Today Commun 2022;33:104494.

[85] Liu X, Lu X, Guan H, Liu X, Wang M, Wang C, et al. Rational design of ZnO/ZnO nanocrystal-modified rGO foam composites with wide-frequency microwave absorption properties. Ceram Int 2021;47:33584–95.
[86] Lu M-M, Cao W-Q, Shi H-L, Fang X-Y, Yang J, Hou Z-L, et al. Multi-wall carbon nanotubes decorated with ZnO nanocrystals: mild solution-process synthesis and highly efficient microwave absorption properties at elevated temperature. J Mater Chem A 2014;2:10540–7.
[87] Li X, Wang L, You W, Li X, Yang L, Zhang J, et al. Enhanced microwave absorption performance from abundant polarization sites of ZnO nanocrystals embedded in CNTs via confined space synthesis. Nanoscale 2019;11:22539.
[88] Wu F, Liu ZH, Xiu T, Zhu BL, Khan I, Liu P, et al. Fabrication of ultralight helical porous carbon fibers with CNTs-confined Ni nanoparticles for enhanced microwave absorption. Compos Pt B-Eng 2021;215:108814.
[89] Sharma A, Kumar R, Gupta A, Agrawal PR, Dwivedi N, Mondal DP, et al. Enhanced electromagnetic interference shielding properties of phenolic resin derived lightweight carbon foam decorated with electrospun zinc oxide nanofibers. Mater Today Commun 2022;30:103055.
[90] Chen Q, Liu X, Wang T, Su X, Liu M, Chaemchuen S, et al. A solvent-free process enabling ZnO/porous carbon with enhanced microwave absorption. J Mater Sci Technol 2023;149:255–64.
[91] Li J, Dai B, Qi Y, Dai Y, Qi Y. Enhanced electromagnetic wave absorption properties of carbon nanofibers embedded with ZnO nanocrystals. J Alloys Compd 2021;877:160132.
[92] Chen C, Wang J, Dong H, Chen W, Zhou K. Facile synthesis of graphite-like carbon nitride/zinc oxide heterojunction for microwave absorption. J Alloys Compd 2023;935:167723.
[93] Skoda D, Vilcakova J, Yadav RS, Hanulikova B, Capkova T, Jurca M, et al. Nickel nanoparticle–decorated reduced graphene oxide via one-step microwave-assisted synthesis and its lightweight and flexible composite with polystyrene-block-poly (ethylene-ran-butylene)-block-polystyrene polymer for electromagnetic wave shielding application. Adv Compos Hybrid Mater 2023;6:113.
[94] Deng J, Wang Q, Zhou Y, Zhao B, Zhang R. Facile design of a ZnO nanorod–Ni core–shell composite with dual peaks to tune its microwave absorption properties. RSC Adv 2017;7:9294–302.
[95] Cheng Y-F, Bi H, Wang C, Cao Jiao W, Che R. Dual-ligand mediated one-pot self-assembly of Cu/ZnO core/shell structures for enhanced microwave absorption. RSC Adv 2016;6:41724.
[96] Zhong B, Tang X, Huang X, Xia L, Zhang X, Wen G, et al. Metal-semiconductor Zn/ZnO core–shell nanocables: facile and large-scale fabrication, growth mechanism, oxidation behavior, and microwave absorption performance. Cryst Eng Comm 2015;17:2806–14.
[97] Jia Z, Kong M, Yu B, Ma Y, Pan J, Wu G. Tunable co/ZnO/C@MWCNTs based on carbon nanotube-coated MOF with excellent microwave absorption properties. J Mater Sci Technol 2022;127:153–63.
[98] Yu Z, Zhou R, Ma M, Zhu R, Miao P, Liu P, et al. ZnO/nitrogen-doped carbon nanocomplex with controlled morphology for highly efficient electromagnetic wave absorption. J Mater Sci Technol 2022;114:206–14.
[99] Peng K, Liu C, Wu Y, Fang G, Xu G, Zhang Y, et al. Understanding the efficient microwave absorption for FeCo@ZnO flakes at elevated temperatures a combined experimental and theoretical approach. J Mater Sci Technol 2022;125:212–21.
[100] Yang J, Guan G, Yan L, Xu J, Xiang J, Zhang K. FeCo/ZnO composite nanofibers for broadband and high efficiency microwave absorption. Adv Mater Interfaces 2021;8:2101047.
[101] Wang J, Jia Z, Liu X, Dou J, Xu B, Wang B, et al. Construction of 1D Heterostructure NiCo@C/ZnO Nanorod with enhanced microwave absorption. Nano-Micro Lett 2021;13:175.
[102] Zeng Z, Wang C, Siqueira G, Han D, Huch A, et al. Nanocellulose-MXene biomimetic aerogels with orientation tunable electromagnetic interference shielding performance. Adv Sci 2020;7(15):2000979.
[103] Shin H, Eom W, Lee KH, Jeong W, Kang DJ, et al. Highly electroconductive and mechanically strong $Ti_3C_2T_x$ MXene fibers using a deformable MXene gel. ACS Nano 2021;15(2):3320–9.
[104] Kong L, Qi J, Li M, Chen X, Yuan X, et al. Electromagnetic wave absorption properties of Ti3C2Tx nanosheets modifed with in-situ growth carbon nanotubes. Carbon 2021;183:322–31.
[105] Huang Y, Xie Y, Zhao J, Yin X, Chai C. Variety of ZIF-8/MXene-based lightweight microwave-absorbing materials: preparation and performances of ZnO/MXene nanocomposites. J Phys Chem C 2022;126:13847–53.
[106] Wang Y-Q, Zhao H-B, Cheng J-B, Liu B-W, Fu Q, Wang Y-Z. Hierarchical Ti3C2Tx@ZnO hollow spheres with excellent microwave absorption inspired by the visual phenomenon of eyeless urchins. Nano-Micro Lett 2022;14:76.
[107] Qian Y, Wei H, Dong J, Du Y, Fang X, Zheng W, et al. Fabrication of urchin-like ZnO-MXene nanocomposites for high-performance electromagnetic absorption. Ceram Int 2017;43:10757–62.
[108] Kong M, Jia Z, Wang B, Dou J, Liu X, Dong Y, et al. Construction of metal-organic framework derived Co/ZnO/Ti3C2Tx composites for excellent microwave absorption. Sustain Mater Technol 2020;26:e00219.
[109] Meng X, Liu Y, Han G, Yang W, Yu Y. Three-dimensional (Fe3O4/ZnO)@C double-core@shell porous nanocomposites with enhanced broadband microwave absorption. Carbon 2020;162:356–64.
[110] Ma W, Yang R, Wang T. ZnO nanorod-based microflowers decorated with Fe3O4 nanoparticles for electromagnetic wave absorption. ACS Appl Nano Mater 2020;3:8319–27.
[111] Wang Z, Wu L, Zhou J, Shen B, Jiang Z. Enhanced microwave absorption of Fe3O4 nanocrystals after heterogeneously growing with ZnO nanoshell. RSC Adv 2013;3:3309–15.
[112] Ren Y-L, Wu H-Y, Lu M-M, Chen Y-J, Zhu C-L, Gao P, et al. Quaternary nanocomposites consisting of graphene, Fe3O4@Fe Core@Shell, and ZnO nanoparticles: synthesis and excellent electromagnetic absorption properties. ACS Appl Mater Interfaces 2012;4:6436–42.
[113] Yin P, Bai H, Zhang L, Wang J, Feng X, Lu C, et al. Broadband electromagnetic dissipation superiority of hierarchical ZnO flakes co-decorated with CoFe/CoFe2O4 and rGO. Ceram Int 2023;49:17680–9.
[114] Gupta S, Sharma SK, Pradhan D, Tai N-H. Ultra-light 3D reduced graphene oxide aerogels decorated with cobalt ferrite and zinc oxide perform excellent electromagnetic interference shielding effectiveness. Compos Part A 2019;123:232–41.
[115] Li F, Zhuang L, Zhan W, Zhou M, Sui G, Zhou A, et al. Desirable microwave absorption performance of ZnFe2O4@ZnO@rGO nanocomposites based on controllable permittivity and permeability. Ceram Int 2020;46:21744–51.
[116] Wang W, Wang Y, Lu Z, Cheng R, Zheng H. Hollow ZnO/ZnFe2O4 microspheres anchored graphene aerogels as a high-efficiency microwave absorber with thermal insulation and hydrophobic performances. Carbon 2023;203:397–409.
[117] Wang Y, Gao X, Wu X, Zhang W, Luo C, Liu P. Facile design of 3D hierarchical NiFe2O4/N-GN/ZnO composite as a high-performance electromagnetic wave absorber. Chem Eng J 2019;375:121942.
[118] Golchinvafa S, Masoudpanah SM, Alamolhoda S. In-situ combustion synthesis of Ni1-xZnxFe2O4/FeNi3/ZnO composite powders for electromagnetic absorption. Ceram Int 2023;49:18134–42.
[119] Zhang L, Lv Y, Ye X, Ma L, Chen S, Wu Y, et al. Polypyrrole decorated flower-like and rod-like ZnO composites with improved microwave absorption performance. Materials 2022;15:3408.
[120] Ye X, Zhang L, Lv Y, Chen D, Chen S, Liu X, et al. Promising broadband and enhanced microwave absorption of polypyrrole decorated hollow porous ZnO microspheres. Phys Scr 2022;97:125827.
[121] Olad A, Shakoori S. Electromagnetic interference attenuation and shielding effect of quaternary epoxy-PPy/Fe3O4-ZnO nanocomposite as a broad band microwave-absorber. J Magn Magn Mater 2018;458:335–45.
[122] Abhilash GP, Sushmita K, Bose S, Shivakumara C. Functionalization of dielectric BaTiO3 and semiconducting ZnO nanoparticles on rGO layers and their polymer composites: applications in EMI shielding. Synth Met 2023;297:117387.
[123] Zuo T, Wang W, Yu D. MXene/ag@ZnO/WPU/melamine gradient composite foams prepared by a unidirectional evaporation approach for absorption-dominated electromagnetic interference shielding. J Alloys Compd 2023;966:171644.
[124] Das P, Katheria A, Nayak J, Das S, Nath K, Ghosh SK, et al. Facile preparation of self-healable and recyclable multilayered graphene-based nanocomposites for electromagnetic interference shielding applications. Colloids Surf A Physicochem Eng Asp 2023;676:132244.
[125] Gupta S, Chang C, Anbalagan AK, Lee C-H, Tai N-H. Reduced graphene oxide/zinc oxide coated wearable electrically conductive cotton textile for high microwave absorption. Compos Sci Technol 2020;188:107994.
[126] Wang S, Li D, Zhou Y, Jiang L. Hierarchical Ti3C2Tx MXene/Ni chain/ZnO array hybrid nanostructures on cotton fabric for durable self-cleaning and enhanced microwave absorption. ACS Nano 2020;14:8634–45.
[127] Han X, Huang Y, Wang J, Zhang G, Li T, Liu P. Flexible hierarchical ZnO/AgNWs/carbon cloth-based film for efficient microwave absorption, high thermal conductivity and strong electro-thermal effect. Compos Part B 2022;229:109458.
[128] Gupta S, Tripathy AR, Tai N-H. Reduced graphene oxide-manganese ferrite/zinc oxide nanorods coated carbonized cotton fabric for absorption-dominant electromagnetic interference shielding. Surf Interfaces 2024;46:103963.